Design, Synthesis, Pharmacology, and In Silico Studies of (1S,2S,3S)-2-((S)-Amino(carboxy)methyl)-3-(carboxymethyl)cyclopropane-1-carboxylic Acid (LBG30300): A Picomolar Potency Subtype-Selective mGlu2 Receptor Agonist

Na Liu, Floriane Eshak, Fanny Malhaire, Isabelle Brabet, Laurent Prézeau, Emma Renard, Jean-Philippe Pin, Francine Acher, Markus Staudt, Lennart Bunch

Design, Synthesis, Pharmacology and In Silico Studies of (1*S*,2*S*,3*S*)-2-((*S*)-Amino(carboxy)methyl)-3-(carboxymethyl)cyclopropane-1-carboxylic acid (LBG30300): A Picomolar Potency Subtype-Selective $mGlu_2$ Receptor Agonist

Na Liu[a], Floriane Eshak[b], Fanny Malhaire[c], Isabelle Brabet[c], Laurent Prézeau[c], Emma Renard[a], Jean-Philippe Pin[c], Francine C. Acher[b], Markus Staudt[a] and Lennart Bunch*[,a]

[a]*Department of Drug Design and Pharmacology, Faculty of Health and Medical Sciences, University of Copenhagen, Denmark*

[b]*Faculty of Basic and Biomedical Sciences, SPPIN CNRS UMR 8003, Université Paris Cité, 75006 Paris, France*

[c]*Institute of Functional Genomics, University of Montpellier, CNRS, Inserm, 34094 Montpellier, France*

*Corresponding authors: Lennart Bunch, E-mail: lebu@sund.ku.dk

ABSTRACT (max 150 words)

The metabotropic glutamate (Glu) receptors (mGlu receptors) play a key role in modulating excitatory neurotransmission in the CNS. In this study, we report the structure-based design and pharmacological evaluation of the densely functionalized, conformationally restricted glutamate analog (1*S*,2*S*,3*S*)-2-((*S*)-Amino(carboxy)methyl)-3-(carboxymethyl)cyclopropane-1-carboxylic acid (**LBG30300**). **LBG30300** was synthesized in a stereo-controlled fashion in nine steps from a commercially available optically active epoxide. Functional characterization at all eight mGlu receptor subtypes showed that **LBG30300** is a picomolar agonist at $mGlu_2$ with excellent selectivity over $mGlu_3$ and the other six mGlu receptor subtypes. Bioavailability studies in mice (IV administration) confirms CNS exposure and an *in silico* study predicts a binding mode of **LBG30300** which induces a flipping of Tyr144 to allow for a salt-bridge interaction of the acetate group with Arg271. The Tyr144 residue now prevents Arg271 to interact with Asp146 which is a residue of differentiation between $mGlu_2$ and $mGlu_3$ and thus could explain the observed subtype selectivity.

INTRODUCTION

The metabotropic Glu receptors (mGlu receptors) are found in the central nervous system (CNS), belong to the class C of G protein-coupled receptors (GPCRs) and are activated by the endogenous agonist (*S*)-glutamate (Glu).[1–3] The eight subtypes, $mGlu_{1\text{-}8}$, are divided into three subgroups based on their sequence homology, cell signaling activation and agonist binding pharmacology.[4] Group I ($mGlu_{1,5}$) are foremost located post synaptically and excitatory in action by coupling to Gq proteins leading to activation of the phospholipase C (PLC) pathway, whereas group II ($mGlu_{2,3}$) and group III ($mGlu_{4,6,7,8}$) are foremost expressed presynaptically and are inhibitory in action, by coupling to Gi/o proteins which leads to inhibition of adenylyl cyclase (AC).[4,5] The group II subtypes, $mGlu_2$ and $mGlu_3$ are differentially distributed in the CNS and exert distinct functions.[5] While $mGlu_{2,3}$ are localized pre- and post-synaptically in neurons,

$mGlu_3$ is also found in glial cells.[6–8] Extensive pharmacological studies suggest that $mGlu_2$ and $mGlu_3$ are associated with several neurological and psychiatric disorders such as cognitive impairment and drug addiction.[9–11]

In order to study and understand the detailed role and function of the $mGlu_2$ and $mGlu_3$ subtypes in CNS disorders, the discovery of pharmacological tools capable of differentiating them are of particular interest. Owing to the high degree of protein sequence homology (70%) between the $mGlu_2$ and $mGlu_3$ receptors with a high residue identity amongst the two orthosteric binding pockets,[12] the discovery of subtype selective orthosteric agonists or antagonists have proved challenging.[13] However the non-conserved Asp146 in $mGlu_2$ which is Ser152 in $mGlu_3$ has structural implications and affects the chloride sensitivity of these receptors.[14] This situation allowed the discovery of $mGlu_{2/3}$ subtype selective ligands.[12]

Taking point in Glu as lead,[15–18,] incorporation of a cyclopropane ring in the 3,4-position of the Glu scaffold, has been explored to give the four diastereomers *L*-2-(carboxycyclopropyl)glycine (*L*-CCG-I–IV).[19] Notably, analog (2*S*,3*S*,4*S*)-2-(2-carboxycyclopropyl)glycine (*L*-CCG-I, Figure 1) was found to be a selective agonist for mGlu receptors with a preference for group II.[19,20] In contrast, *L*-CCG-II is only a weak agonist at the mGlu receptors with EC_{50} of 300 μM at $mGlu_2$.[21] DCG-IV is also a fairly potent agonist at $mGlu_2$ with 4-fold higher potency at $mGlu_3$.[22] Replacement of one of the distal carboxylate groups in DCG-IV with a methyl group, *L*-CCG-I analog (2*S*,3*S*,4*S*,4′*R*)-2-(2-carboxy-3′-methylcyclopropyl) glycine (**1a**), was obtained. This change significantly enhances agonist potencies (~40 fold), but low discrepancy between $mGlu_2$ over $mGlu_3$ remained.[23] A hydroxymethyl group in the very same position, compound **1b**, did not improve this.[24]

Recently we have shown that addition of a methyl group in the 4*R*-position of the weak mGlu receptor agonist *L*-CCG-II (**1c**, Figure 1), significantly enhances agonist potency (~3500 fold, to EC_{50}= 82 nM) and induce selectivity for $mGlu_2$ over $mGlu_3$ (~15 fold).[25]

Early on, researchers at Eli Lilly and Company designed and synthesized a series of bicyclic amino acid analogs, in which the Glu skeleton was incorporated into a fused bicyclo[3.1.0]hexane frame and perfectly mimics the extended conformation of Glu also found when crystallized with the mGlu-ligand binding domain (LBD). The constrained bicyclic amino acid (1*S*,2*S*,5*R*,6*S*)-2-aminobicyclo[3.1.0]hexane-2,6-dicarboxylate (**2a**, LY354740, Figure 1) possessed high potency and selectivity for $mGlu_{2/3}$.[26] Further studies disclosed that a methyl group in the C4α-position of **2a** led to the highly potent $mGlu_2$ agonist (1*S*,2*S*,4*R*,5*R*,6*S*)-2-amino-4-methylbicyclo[3.1.0]hexane-2,6-dicarboxylic acid (**2b**, LY541850, Figure 1) with partial agonist/antagonist activity at $mGlu_3$.[27,28] The analog (1*R*,2*S*,4*R*,5*R*,6*R*)-2-Amino-4-(1*H*-1,2,4-triazol-3-ylsulfanyl)bicyclo[3.1.0]hexane-2,6-dicarboxylic acid (**2c**, LY2812223, Figure 1) with a thiotriazole group at this same position was reported as a functionally selective $mGlu_2$ agonist.[28,29] Furthermore, (1*S*,2*S*,4*S*,5*R*,6*S*)-2-amino-4-[(3-methoxybenzoyl)amino]bicyclo[3.1.0]hexane-2,6-dicarboxylic acid (**2d**, LY2794193, Figure 1) with (3-methoxybenzoyl)amino substitution at the C4β-position was recently demonstrated to be a highly potent $mGlu_3$-selective agonist.[30]

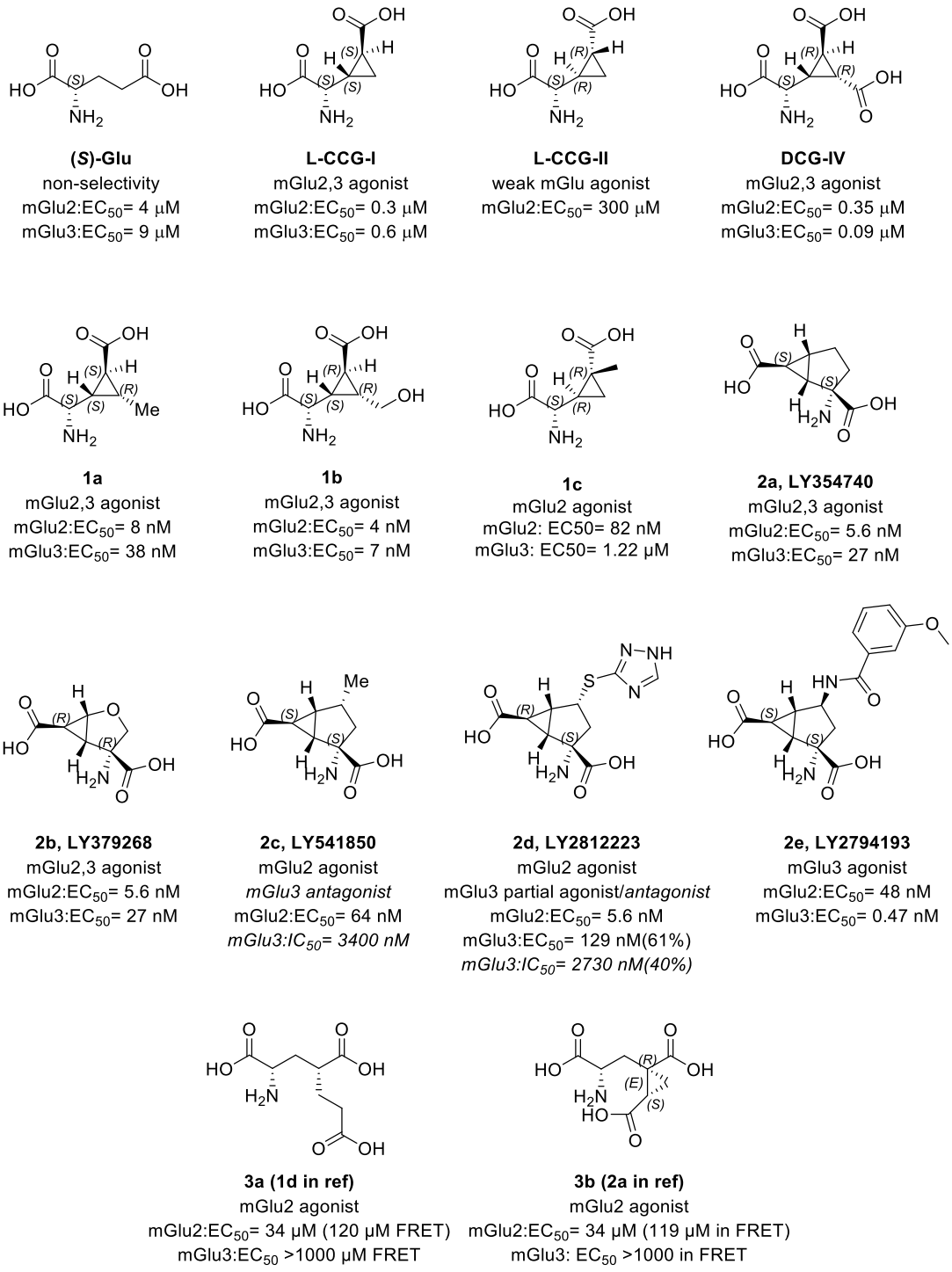

Figure 1. Chemical structures of endogenous agonist (*S*)-Glu, and synthetic analogs DCGIV, *L*-CCG-I, *L*-CCG-II, L-CCG-I analogs **1a,b**, L-CCG-II analog **1c**, fused bicycles **2a-e**, and Glu analogs **3a,b**. All data from functional assays except for FRET.

RESULTS AND DISCUSSION

Design

It is well-known from crystal structures and modeling studies[31,32] that Glu binds to mGlu receptors in an extended conformation and that key interactions of the distal carboxylate group with the receptor are salt-bridges to Arg61 and Lys377 ($mGlu_2$ numbering). Docking of conformationally restricted Glu analog L-CCG-I (Figure 2A) follows this convention, and the enhanced potency (μM to nM) is believed to be a result of reduced entropic loss on binding as well as its slightly enhanced hydrophobic nature.

L-CCG-II is a very weak mGlu agonist, but most recently we have reported that the 4-methyl analog, compound **1c**, is a nanomolar-potent and selective $mGlu_2$ agonist.[25] Interestingly, docking of **1c** into $mGlu_2$ (Figure 2B) suggests an alternative binding mode to Glu, wherein the distal carboxylate group forms a salt-bridge to both Arg61 and Arg57, but not Lys377. Additionally, the methyl group of **1c** allows a hydrophobic interaction with Tyr144.[25] Since both Arg57 and Tyr144 are signature residues for group II (Table S1), we believe this could explain the group II selectivity of **1c**. However, the observed ~15-fold selectivity for $mGlu_2$ over $mGlu_3$ cannot be explained herefrom.[25]

DCG-IV may also be categorized as an analog of L-CCG-I and docking into $mGlu_2$ (Figure 2C) reveals a strong hydrogen bond to Ser272 and a salt-bridge to Arg57 from the added carboxylate group.

We have previously reported that syn-2,4-substituted Glu analog **3a** is a selective $mGlu_2$ agonist and also its conformationally restricted analog **3b**, however, both in micromolar potency.[33] Docking of **3a** into $mGlu_2$ (Figure 2D) shows that the distal carboxylate engages in a salt-bridge with Arg61/Lys377, while the sidechain carboxylate group engages in a salt-bridge with Arg57 and a hydrogen bond with Ser272. Notably is that the Glu backbone in **3a** adopts an extended conformation which is not a low-energy conformation of this compound among the numerous conformations it can adopt due to the high number of rotatable bonds (ligand flexibility ->

entropic loss on binding). Together we suspect this situation to be the reason for the low potency of **3a**.

With this analysis in mind, we set out to design a Glu analog which holds an additional carboxylate group which can engage in strong salt-bridge interaction with Arg57 and a hydrogen bond to Ser272. Also, hydrophobic interactions to Tyr144 would be desirable, as all of these three residues are characteristic for group II mGlu receptors (Table S1). The backbone Glu should adapt an extended low-energy conformation and engage strongly with the receptor as what is known for Glu itself.

After a number of iterative explorative rounds of design, wherein we explored different functional groups and carbon chain lengths, we identified densely functionalized, conformationally restrained L-CCG-I analog **LBG30300** (Figure 3). From a retrosynthetic perspective, **LBG30300** also seemed to be a task that could be accomplished in a reasonable time frame. **LBG30300** holds a (5*S*)-acetate group as the additionally interacting group and a quick docking of **LBG30300** into $mGlu_2$ (Figure 4) shows that this acetate group readily engages in a salt-bridge with Arg57 and a strong hydrogen bond to Ser272. Also, **LBG30300** adopts a Glu-like backbone conformation optimizing all Glu-like interactions with the receptor. Lastly, **LBG30300** is highly conformationally restricted compared to **3a**, which would call for enhanced potency, however, the $mGlu_{2/3}$ subtype selectivity of **LBG30300** cannot be concluded here from.

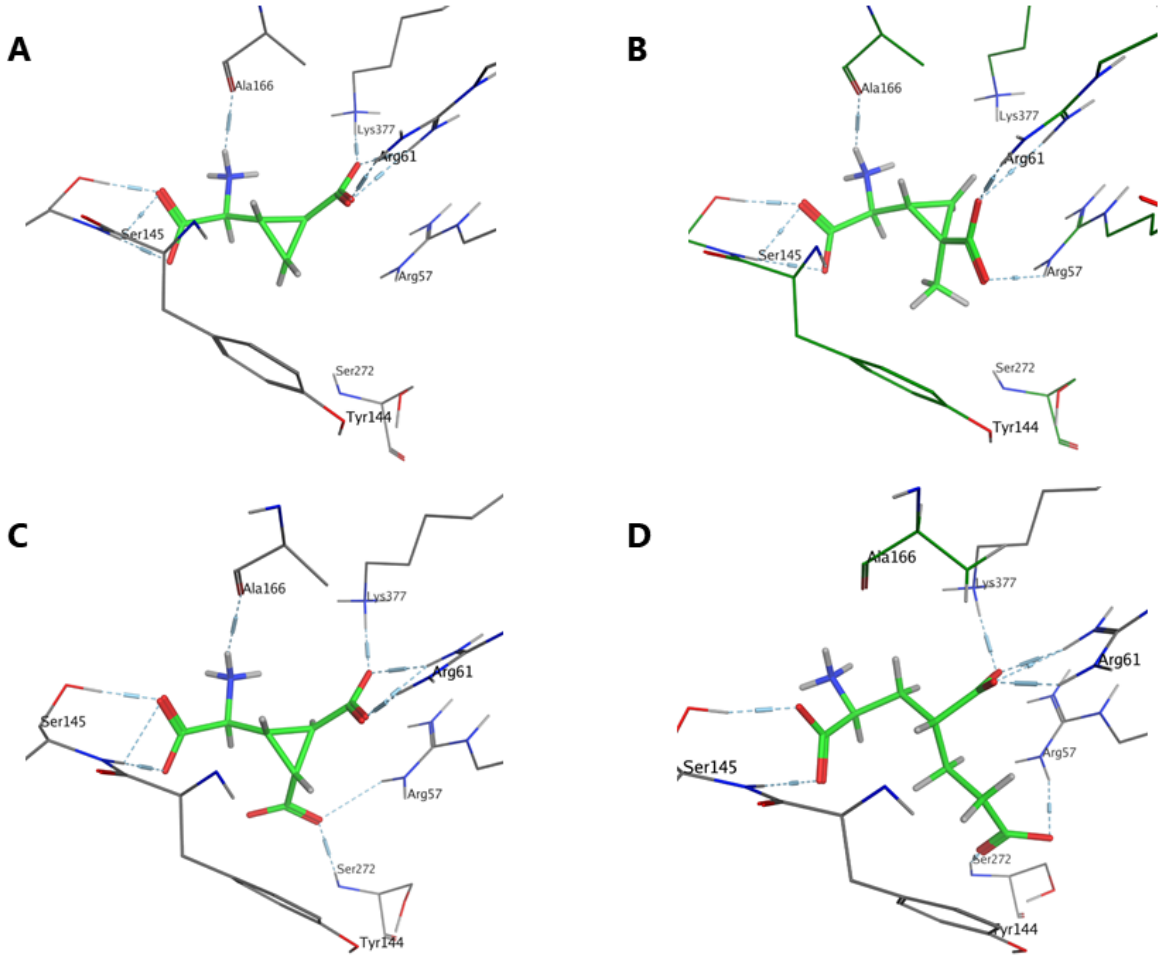

Figure 2. Induced-fit docking in MOE (standard setup). **A**) L-CCG-I (green) into mGlu$_2$-VFT (pdb code 5CNI) (free energy of binding, *S*= -7.5 kcal/mol). The distal carboxylate group forms dual salt-bridge interactions with conserved Arg61/Lys377 but not group II characteristic Arg57/Ser272/Tyr144. **B**) **1c** (green) into mGlu$_2$-VFT (pdb code 5CNI) (free energy of binding, *S*= -7.2 kcal/mol). The distal carboxylate group forms dual salt-bridge interactions with conserved Arg61 and group II characteristic Arg57 (but not conserved Lys377), while the methyl group engages in a Π-alkyl contact with Tyr144. **C**) DCG-IV into mGlu$_2$-VFT (pdb code 5CNI) (free energy of binding, *S*= -8.4 kcal/mol). The distal carboxylate group engages in dual salt bridge interactions with Arg61/Lys377 while the non-Glu carboxylate group engages in a salt bridge with Arg57 and a hydrogen bond interaction with Ser272. This binding mode is comparable to observed of DCG-IV when crystallized in mGlu$_3$-VFT (PDB ID 2E4V). **D**) 4-Substituted Glu analog **3a** (green) in mGlu$_2$-VFT (pdb code 5CNI) (free energy of binding, *S*= -7.6 kcal/mol). The distal carboxylate engages in salt bridge with Arg61/Lys377, while the sidechain carboxylate group engages in a salt-bridge with Arg57 and a hydrogen bond with Ser272.

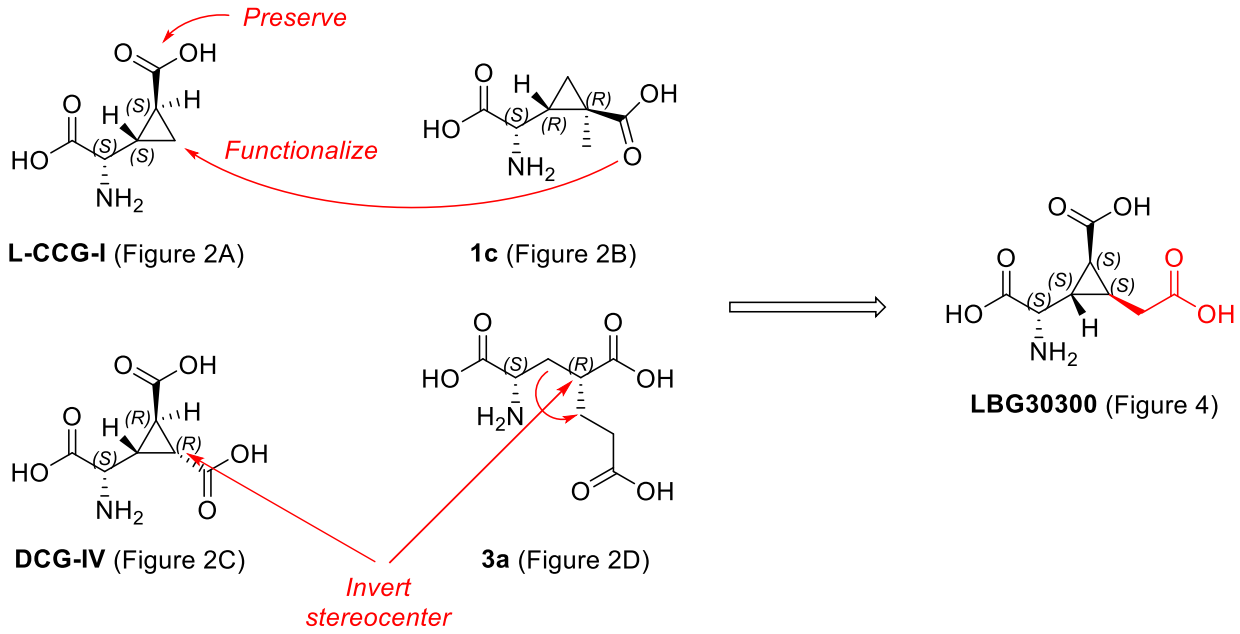

Figure 3. Structural considerations and strategy behind design of densely functionalized L-CCG-I analog **LBG30300**.

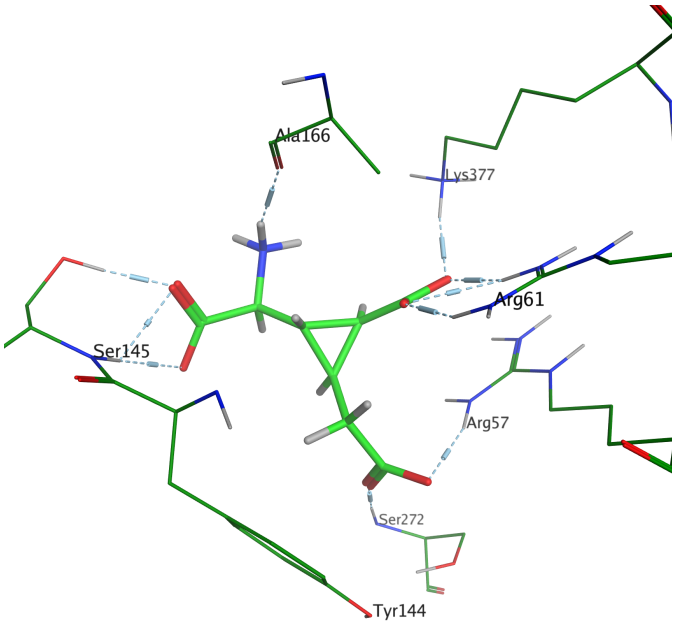

Figure 4. Induced-fit docking in MOE (standard setup) of **LBG30300** into mGlu$_2$-VFT (pdb code 5CNI) (free energy of binding, *S*= -8.4 kcal/mol). The distal carboxylate group forms a salt-bridge interaction with Arg61/Lys377, similarly to Glu. The 5*S*-acetate group engages in salt-bridge interaction with Arg57 and in hydrogen bond interaction with the backbone NH of Ser272. Arg57 and Ser272 are both characteristic for group II receptors (mGlu$_{2/3}$).

Chemistry

Four chiral center, densely functionalized Glu analog **LBG30300** presents a synthetic challenge notably with the *cis* and dual *trans* relationships around the cyclopropane ring together with the adjacent chirality at the alpha amino acid position. Thus, a retrosynthetic analysis suggested a stereospecific synthesis starting from commercially available chiral epoxide (*S*)-glycidol benzyl ether **5** with a key C-H activation step for the selective *cis*-introduction of the acetic acid functionality on the cyclopropane ring. The synthesis (Scheme 1) began with a Wadsworth-Emmons cyclopropanation reaction of **5** with triethyl phosphonoacetate and *n*-BuLi in dimethoxyethane at 130 °C, to give enantiomerically pure *trans*-cyclopropane carboxylic ester **6** in 79% yield.[34] After, hydrolysis with LiOH gave acid **7** and following amide coupling with 8-aminoquinoline in the presence of EDCI and HOBt, intermediate **8** was obtained in 68% yield. The key C-H activation-alkylation on cyclopropane **8** was performed with ethyl iodoactetate, $Pd(OAc)_2$ as the Pd catalyst and AgOAc as base in toluene for refluxing over 3 days to give the desired product **9** in 46% yield.[35] Removal of the benzyl ether protecting group of **9** failed under standard H_2 and Pd/C conditions presumably due to presence of the nitrogen containing bidentate directing group. Alternatively, the benzyl ether was removed by applying the Lewis acid BCl_3 at −78 °C for 1.5 h to successfully give the free alcohol **10** in 75% yield. Oxidation by Dess-Martin periodinane (DMP) afforded aldehyde **11** in 60% yield. For the installation of the amino acid moiety, the asymmetric Strecker reaction was applied to aldehyde **11** with the chiral auxiliary (*R*)-α-phenylglycinol to give the Schiff base, which was treated with TMSCN *in situ* to give the expected diastereomeric α-aminonitrile derivative **12** in 62% yield.[36,37] The α-aminonitrile **12** was then submitted to oxidative cleavage with lead tetraacetate, followed by refluxing in 6 M HCl for overnight to hydrolyze the ester and nitrile, and cleavage of the directing group 8-

aminoquinoline at the same time. The target compound **LBG30300** was obtained as the HCl salt by preparative HPLC in 20% yield.

Scheme 1. Stereoselective synthesis of densely functionalized L-CCG-I analog **LBG30300**[a]

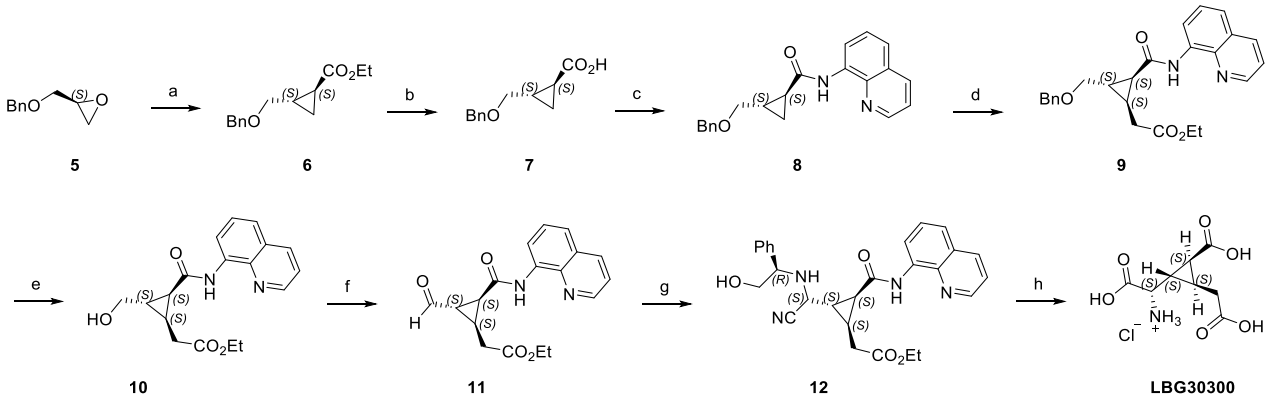

[a]*Reagents and conditions*: (a) Triethyl phosphonoacetate, *n*-BuLi, dimethoxyethane, 130 °C, overnight, 79%; (b) NaOH(aq), THF, rt, overnight, quant.; (c) 8-Aminoquinoline, EDCI, HOBt, DCM, rt, 4 d, 68%; (d) ICH_2COOEt, $Pd(OAc)_2$, AgOAc, toluene, 110 °C, 3 d, 46%; (e) BCl_3, $NaHCO_3$, DCM, -78 °C to 0 °C, 75%; (f) DMP, DCM, rt, overnight, 60%; (g) (*R*)-α-phenylglycinol, MeOH, rt, 3 h; then TMSCN, rt, overnight, 62%; (h) i. $Pb(OAc)_4$, DCM, MeOH, 0 °C, 10 min; ii. 6 M HCl, 110 °C, overnight, 20% over two steps.

Pharmacological characterization

With densely functionalized cyclopropane **LBG30300** in hand, it was characterized for both agonist- and antagonist activity at rat $mGlu_{1-8}$ in an IP-One functional assay (Table 1). For the antagonist activity, the compounds were tested for their capacity to inhibit the responses mediated by an EC80 agonist concentration (Quisqualate 0.3 and 0.1 μM for $mGlu_1$ and $mGlu_5$ receptors, LY379268 3 nM for $mGlu_2$ and $mGlu_3$ receptors, and L-AP4 at 1, 10, 1000 and 1 μM for $mGlu_{4,6,7,8}$). Most satisfyingly, **LBG30300** displays sub-nanomolar agonist potency at $mGlu_2$ (EC_{50}= 0.6 nM), with a >100-fold selectivity over $mGlu_3$ (EC_{50}= 0.373 μM). Also, more than 50.000-fold selectivity over group I subtypes $mGlu_{1,5}$ and a ~160 to >50.000-fold selectivity over

group III subtypes $mGlu_{4,6,7,8}$ was observed. No antagonist activity was observed for any of the $mGlu_{1\text{-}8}$ subtypes.

In comparison with already reported selective $mGlu_2$ agonists this is an impressive potency and subtype selectivity ratio.

Table 1. Pharmacological characterization at rat $mGlu_{1-8}$ by IP-One functional assay[a]

Compound	Group I		Group II		Group III			
	$mGlu_1$ EC_{50} (pEC_{50})	**$mGlu_5$ EC_{50} (pEC_{50})**	**$mGlu_2$ EC_{50} (pEC_{50})**	**$mGlu_3$ EC_{50} (pEC_{50})**	**$mGlu_4$ EC_{50} (pEC_{50})**	**$mGlu_6$ EC_{50} (pEC_{50})**	**$mGlu_7$ EC_{50} (pEC_{50})**	**$mGlu_8$ EC_{50} (pEC_{50})**
Quisqualate	0.079 (7.22 ± 0.20)	0.027 (7.39 ± 0.17)	--	--	--	--	--	--
LY379268	--	--	0.001 (9.02 ±0.08)	0.010 (8.00 ± 0.19)	--	--	--	--
LAP4	--	--	--	--	0.18 (6.76 ± 0.09)	2.5 (5.64 ± 0.08)	~100%@ 3000 µM	0.29 (6.76 ± 0.18)
1c, LBG30120SRR	5.50 (5.29 ±0.09)	12.0 (4.95 ±0.10)	0.082 (7.09 ±0.04)	1.88 (5.73 ±0.06)	>>30	2.50 (5,67 ±0.02)	>30	>30
LBG30300	>30	>30	0.0006 (9.24 ±0.07)	0.373 (6.43 ±0.10)	0.11 (-7.45 ±0.27)	0.28 (6.61 ±0.06)	>30	0.097 (7.45 ±0.27)

[a]As group-II and group-III mGlu receptors are naturally coupled to Gi, they were co-expressed with the chimeric Gqi9 protein to allow them to activate PLC and produce IP1. EC_{50} values in µM, pEC_{50}±pSEM in parentheses, or in percent activation at the indicated single-dose stimulation comparing to references (Quis for $mGlu_{1,5}$; LY379268 for $mGlu_{2,3}$; LAP4 for $mGlu_{4,6\text{-}8}$). Mean values calculated from 2 to 5 experiments. --, not tested. All responses are full agonist responses, and are presented in Supp Fig XXX. No antagonistic effect could be observed for any of the tested compounds.

Table 2. Comparison of key mGlu agonists with **LBG30300** across different functional assays

	$mGlu_2$	**$mGlu_3$**	**$mGlu_2$**	**$mGlu_3$**	**$mGlu_2$**	**$mGlu_3$**	**$mGlu_{2/3}$**
	cAMP		Ca^{2+} FLIPR		IPOne		Ratio[a]
LY354740[29]	7.0	28	34	140	--	--	4 / 4 / --
LY379268[29,38]	1.1	1.1	4.0	15	1	10	1 / 5 / 10
LY404039[39]	23	48	--	--	--	--	2 / -- / --
LY2812223[29]	5.6	129 *(2730)*	21	>25000 *(25200)*	--	--	23 / 1200 / --

LBG30300	--	--	--	--	0.6	372	--/--/~620

All values are EC_{50} in nM. --: data not available. Numbers in parentheses/italic are antagonist functional responses. Agonist potencies in the Ca^{2+} and IPOne assays were determined after co-expression of the indicated receptor with the chimeric Gqi9 protein that allows these Gi-coupled receptors to activate phospholipase C. Values for the LY compounds were taken from the indicated references.

[a] Ratios calculated from the three assays separated by '/'

FRET assay

For many reported $mGlu_2$-selective agonists, the selectivity is based on a functional response, while when determining $mGlu_2/mGlu_3$ binding affinity, the selectivity ratio is significantly lower (Table 2). In the absence of a radioligand, we decided to investigate further the $mGlu_2/mGlu_3$ selectivity of **LBG30300** in a non-functional conformational FRET-based assay.[40,41] The assay relates on the reorientation of the VFTs that occurs upon agonist binding, and potencies measured for agonists were closer to their binding affinity due to the absence of potentiating effect of the G proteins for most receptors in living cells.[40] It is well-established that Glu has a higher affinity to $mGlu_3$, such that it was not possible to prevent any agonist action of ambient glutamate, leading to most $mGlu_3$ receptors already in active form. We therefore pre-incubated the cells with the antagonist **LY341495** (0.3 μM) to prevent basal action of ambient glutamate. Agonist dose-response curves were then performed in cells expressing $mGlu_2$ or $mGlu_3$ for comparison after antagonist pre-incubation, and with $mGlu_2$ cells without antagonist pre-incubation. Results are presented in Table 3.

While the $mGlu_{2/3}$ ratio of **LY354740** in binding affinity studies is around 1.5, we determine it to be 21 in the FRET assay. For **LBG30300**, the FRET-based $mGlu_{2/3}$ ratio is an impressive 513-fold in favor of $mGlu_2$. On this basis, we conclude that **LBG30300** binds to $mGlu_2$ with a ~40-fold selectivity ratio over $mGlu_3$, and thus candidate for the development into an $mGlu_2$ PET tracer.

Table 3. Comparison of binding affinities and FRET data

	$mGlu_2$	$mGlu_3$	$mGlu_{2/3}$ ratio	FRET $mGlu_2$		FRET $mGlu_2$ pre-incubation with antagonist		FRET $mGlu_3$ pre-incubation with antagonist		$mGlu_{2/3}$ ratio
	[^{3}H]LY341495			EC_{50}	pEC_{50} ±pSEM	EC_{50}	pEC_{50} ±pSEM	EC_{50}	pEC_{50} ±pSEM	
LY354740	0.072	0.107	1.5	0.063	-7.20 ±0.01	0.229	-6.64 ±0.08	4.800	-5.32 ±0.06	21
LY2794193	--	--		2.818	-5.55 ±0.13	-	-	0.032	-7.50 ±0.12	
LBG30300	--	--		0.013	-7.90 ±0.07	0.022	-7.65 ±0.09	11.500	-4.94 ±0.09	513

EC_{50} values in μM

Bioavailability

With the pharmacological profile in hand, we determined the bioavailability profile of **LBG30300** in rodent, including plasma-brain distribution over time. **LBG30300** was administered IV in mice (10 mg/kg), and results summarized in Table 4. While **LBG30300** shows high bioavailability with a plasma C_{max} of 5365 ng/mL, it has a rapid plasma half-life of ~30 min. **LBG30300** enters the brain with a max concentration of 86 ng/g and shows a longer half-life. Plasma protein- and brain tissue binding for **LBG30300** was determined at 53% ±0.4 and 80% ±8.5, respectively and from these data. Kp,uu (AUC) was following calculated at 0.02.

Table 4. Bioavailability of **LBG30300** in mice, compared with reference compounds **LY354740** and **LY544344** (prodrug of LY354740).[42]

Compound	*Dose (route of administration)*	*Time (h)*	*Plasma Cmax [ng/mL]*	*Brain Cmax [ng/g]*	*CSF Cmax [ng/g]*	*t½ (h) plasma/brain*	*Kp,uu (AUC)*
LY354740	100 mg/kg (PO)	--	2120	76	14	6.8 / 69	
LY544344	10 mg/kg (PO)	--	3300	85	24	4.4 / 74	
LBG30300	10 mg/kg (IV)	0.25	5365 ±514	86 ±14	--	~0.5 / --	0.02
LBG30300	10 mg/kg (IV)	1.0	583 ±232	75 ±12	--		
LBG30300	10 mg/kg (IV)	4.0	50 ±6.6	68 ±11	--		

--: data point not available

Molecular Modeling

LBG30300 displays a remarkable pico-molar potency at $mGlu_2$ and selectivity over $mGlu_3$ and other mGlu receptor subtypes. This compound is a substituted derivative of L-CCG-I for which the cyclopropyl ring increases the glutamate potency to the sub-µM range at group-II mGlu receptor subtypes.[12] Further potency and selectivity of **LBG30300** are brought by the additional acetate substituent. Indeed, dockings at the glutamate binding site of these subtypes provide an interpretation of such properties (Figure 4). Yet the subtype selectivity between $mGlu_2$ and $mGlu_3$ cannot be explained with the first basic docking experiments (Figure 4).

Since an $mGlu_2$ selective agonist **LY2812223** has been described and a 3D-structure of this compound bound to the glutamate binding domain named Venus Flytrap domain (VFT) made available (PDB ID 5CNJ)[29], we chose this structure as template.

Docking of **LBG30300** was performed using Gold[43] as implemented in Discovery Studio. The stability of the complex was assessed by molecular dynamics simulations. Besides the interactions of the amino acid moiety of **LBG30300** with the common signature motif[44] (Figure S1), four basic and one hydrophilic residues make polar bindings with the two distal carboxylates of **LBG30300** (Arg57, Arg61, Arg271, Ser272 and Lys377, Figure 5). Whereas Arg61 and Lys377 are conserved residues across the eight mGlu receptors, Arg57, Arg271 and Ser272 are group II ($mGlu_2$ and $mGlu_3$) selective (Table S1). In addition, Tyr144 is also group-II selective (Table S1). Of notice, Tyr144 adopts a flipped conformation in the 5CNJ structure (chain A) where **LY281223** is bound to $mGlu_2$ compared to its conformation in 5CNI where glutamate is bound to $mGlu_2$ as described by Monn et al.[29] Indeed this flipped Tyr144 allows the docking of compound **LBG30300** in the 5CNJ chain A template (Figure 5). Docking of **LBG30300** in the $mGlu_2$ 3D-model with non-flipped Tyr144 (5CNJ chain B) with flexible residues at the binding site also results in flipping of Tyr144 and a binding mode of **LBG30300** as obtained for docking into chain A (Figure 5 and S1).

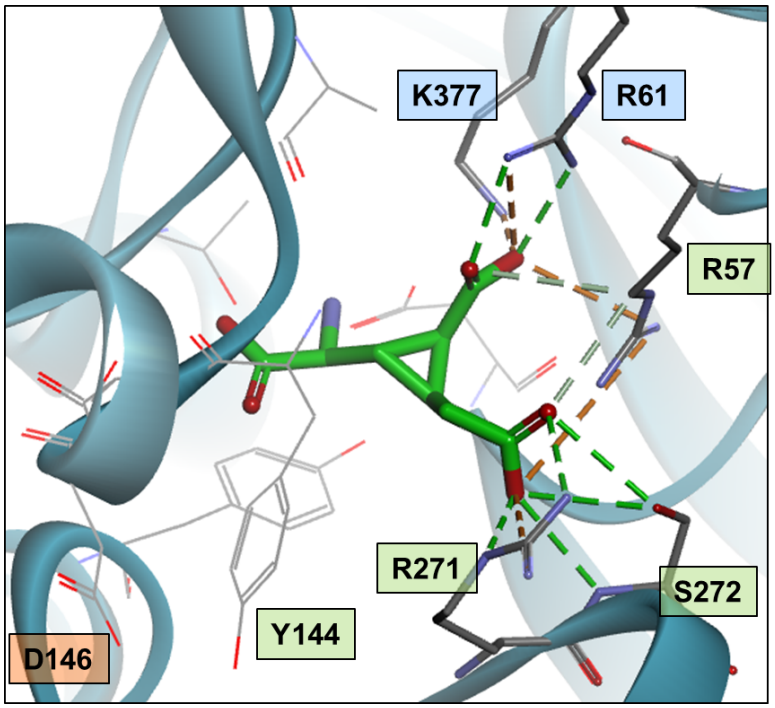

Figure 5. Docking of **LBG30300** at $mGlu_2$ receptor binding site. Distal interactions are displayed as dashed lines (green H-bonds, brown salt bridges, hydrogens omitted for clarity). The five distal polar binding residues are displayed in sticks and labeled as well as Tyr144 and D146. These residues are boxed and colored as in Table S1 (blue, green and orange for conserved, group-II and subtype selective residues respectively). Proximal binding residues are indicated in Figure S1. Atom colors: C green for ligand, gray for residue side chains, O red, N blue.

The docking of **LBG30300** at $mGlu_2$ receptor binding site reveals that the flip of Tyr144 allows a salt bridge and a hydrogen bond between the acidic function of the acetate group of **LBG30300** and Arg271 and Ser272 (Figure 5 and 4). In this case, Arg271 has lost its salt bridge with Asp146, which is a selective residue between $mGlu_2$ and $mGlu_3$ (Ser152) but gained a hydrophobic contact with Tyr144 (Figure 6). We have previously described this $mGlu_2$ selective interaction between Asp146 and Arg271.[14] Asp146 remains bound to the inferior lobe of the VFT through an ionic interaction with Arg243. The consequences of the Tyr144 flip on the Arg271 interactions are illustrated in Figure 7.

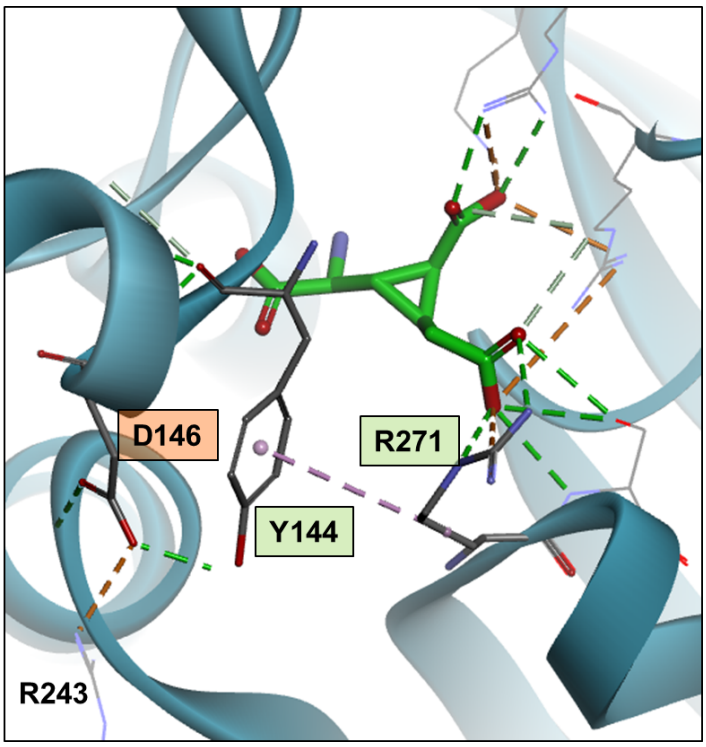

Figure 6. Docking of **LBG30300** at the $mGlu_2$ receptor binding site showing the flipped Tyr144 and Arg271 interacting with **LBG30300** and no longer with Asp146.[14] D146, Y144 and R271 (sticks) are boxed and colored according to selectivity as in Table S1. Interactions displayed as described in Figure 5 (hydrophobic contact in mauve).

A)

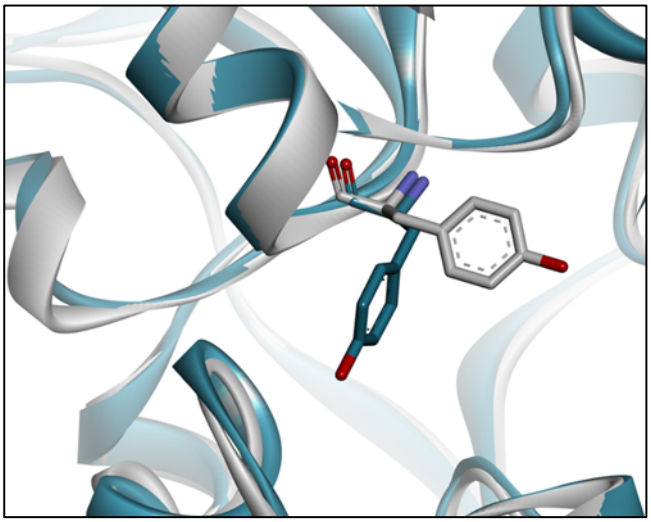

B)

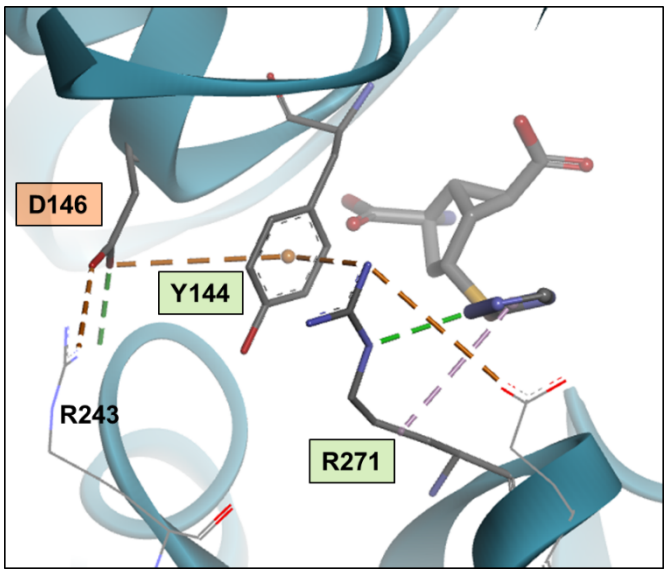

C)

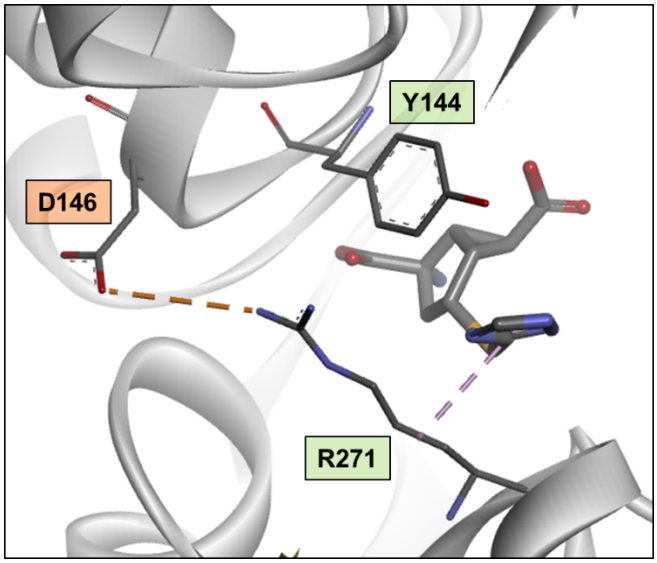

Figure 7. Tyr144 in 5CNJ ($mGlu_2$ bound to LY2812223). A) Superimposition of chain A (green-blue, flipped Tyr144) and chain B (gray, non-flipped Tyr144) of 5CNJ showing the change in spatial orientation of the Tyr144 side chain. B) Flipped Tyr144 in chain A preventing Arg271 to interact with Asp146. C) non flipped Tyr144 in chain B, allowing Arg271-Asp146 interaction. Asp146, Tyr144 and Arg271 are displayed as thin sticks, their labels colored as in Table S1 in panel B and C. The ligand LY2812223 is displayed in sticks in panel B and C.

We next proceeded to the docking of **LBG30300** at $mGlu_3$ binding site using the crystal structure of $mGlu_3$ VFT bound to **LY354740** (PDB ID 4XAR, Figure 8).[28] The highest docked pose

showed that Tyr150 did not flip preventing Arg277 homologous to Arg271 in $mGlu_2$, to interact with **LBG30300**. As seen for other $mGlu_3$ agonists (glutamate and **LY354740**, PDB ID 5CNK and 4XAR), Arg277 interacts with Ser152 through an intermediate halide.[14] In this situation, the acetate group of **LBG30300** interacts with Arg64 and Ser278 but is not making any additional stabilizing interactions with Arg277 and the compound displays a weaker activity compared to that at $mGlu_2$ in the μM range. Thus, the $mGlu_{2/3}$ selectivity of **LBG30300** may be explained by its selective interaction with Arg271 when Tyr144 is flipped in $mGlu_2$ which is not possible with homologous Arg277 in $mGlu_3$.[14] In $mGlu_3$ the interaction between Ser152 (upper lobe of the VFT) and Arg277 (lower lobe of the VFT) mediated by a halide ion cannot be offset as between Asp146 and Arg271 in $mGlu_2$ where Asp146 can make new interactions with the lower lobe of the VFT (Arg243 and Asp215 backbone) (Figures 4 and 6).

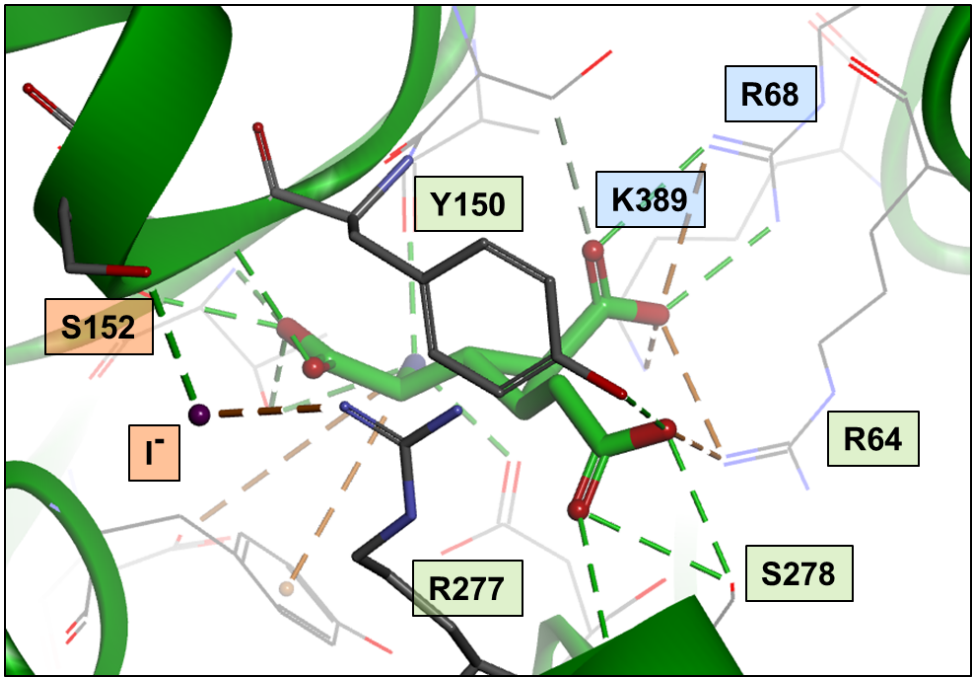

Figure 8. Docking of **LBG30300** at the $mGlu_3$ receptor binding site (PDB ID 4XAR). Proximal and distal interactions are displayed as dashed lines (green H-bonds, brown salt bridges, hydrogens omitted for clarity). The four distal polar residues are labeled as well as Arg277 and Tyr150. Residues involved in group-II and subtype ($mGlu_2$ versus $mGlu_3$) selectivity are boxed and colored as in Table S1. The halide (iodide) bridging Arg277 and Ser152 is displayed as a purple sphere.

LBG30300 is also quite potent at $mGlu_{4, 6}$ and $_{8}$ receptors (Table 1). Indeed, the additional distal acidic function of glutamate analogues (e.g. LAP4, ACPT-1, DCPG) is the hallmark of group-III mGlu receptors. This increased potency has been explained by the highly basic distal environment due to four basic residues.[12] **LBG30300** is most potent at $mGlu_8$, so we docked it in the X-ray structure of the binding domain bound to glutamate (PDB ID 6BSZ, Figure 9). The docking reveals that the two distal carboxylates of **LBG30300** make salt bridges with the four basic residues of the distal binding site (Lys71, Arg75, Lys314, Lys401). Although similar polar interactions occur at $mGlu_2$ and $mGlu_8$ with four distal basic residues, the increased potency of **LBG30300** at $mGlu_2$ may be due to larger van der Waals (including hydrophobic) contacts at $mGlu_2$ (Figure S2 and S3).

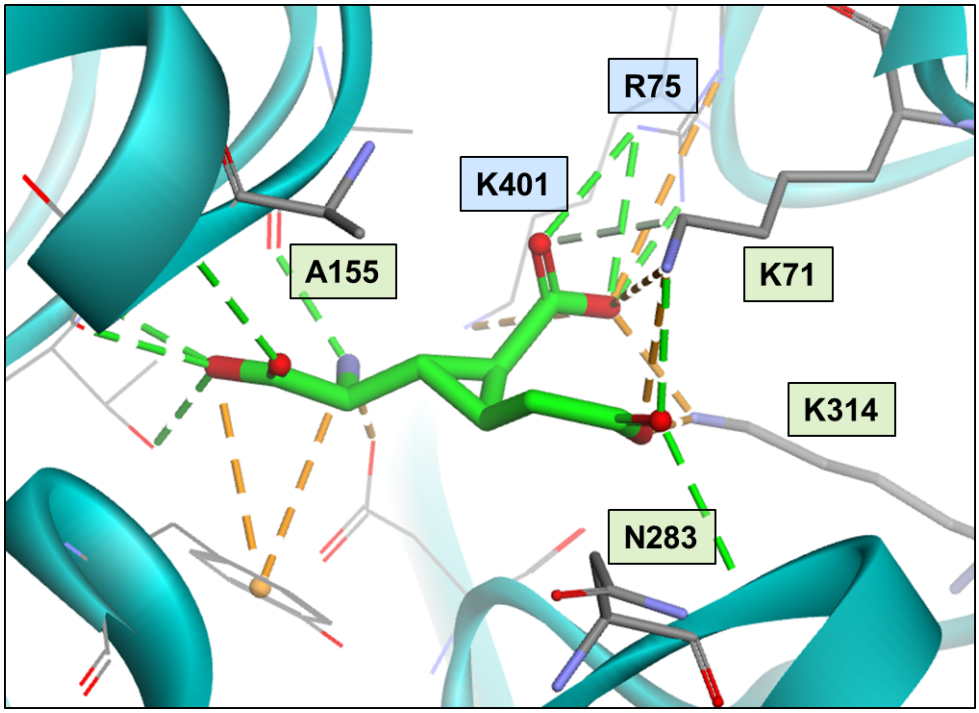

Figure 9. Docking of **LBG30300** at the $mGlu_8$ receptor binding site ((PDB ID 6BSZ). Proximal and distal interactions are displayed as in **Figure 5**. Residues involved in selective binding (sticks) at $mGlu_2$ or $mGlu_8$ are boxed and colored as in Table S1.

CONCLUSION

In conclusion we applied structure-based design to propose a new densely functionalized analog of L-CCG-I as a potential $mGlu_2$ agonist. Its stereoselective synthesis was accomplished in nine steps with a stereospecific CH-insertion of an acetate group, as the key step. Pharmacological characterization of **LBG30300** showed a staggering picomolar potency at $mGlu_2$ in an IPOne functional assay, but also a >100 fold selectivity over $mGlu_3$. An *in silico* study was carried out to address this impressive subtype selectivity in details, and a vital role of residues Tyr144, Arg57, Asp146 and Arg271 in stabilizing the closed conformation of $mGlu_2$ orthosteric binding pocket, is suggested to be the origin of the observed selectivity for $mGlu_2$ over $mGlu_3$. A bioavailability study in mice shows that **LBG30300** crosses the BBB and in combination with data from a FRET-based assay, leads us to conclude that **LBG30300** is a promising candidate for development of an orthosteric $mGlu_2$ PET tracer.

EXPERIMENTAL SECTION

Chemistry

All reactions involving dry solvents or sensitive agents were performed under an argon atmosphere and glassware was flame dried under vacuum prior to use. Commercially available chemicals were used without further purification. DCM, THF and DMF were dried using a SG WATER solvent purification system (commercialized by Pure Process Technology). MeOH was dried by standing over 4 Å molecular sieves for a minimum of 48h. Reactions were monitored by analytical thin-layer chromatography (TLC, Merck silica gel 60 F_{254} aluminum sheets) or by HPLC. Flash chromatography was carried out using Merck silica gel 60A (40-63 μm). For dry column vacuum chromatography (DCVC), Merck silica gel 60 (15-40 μm) and a standard setup was used. ^{1}H NMR spectra were recorded at 400 or 600 MHz and ^{13}C NMR spectra at 100 or 150 MHz on a Bruker Avance III or Bruker Avance III HD, respectively. Chemical shifts (δ) are reported in ppm relative to TMS. For ^{13}C NMR in D_2O was added 1% CD_3OD as internal reference. HPLC was performed using a Dionex UltiMate 3000 pump and photodiode array detector (210 and 254 nm, respectively) installed with an XTerra MS C 18 3.5 μ m, 4.6 mm × 150 mm column, using a 5 → 95% MeCN gradient in H_2O containing 0.1% TFA. For HPLC control, data collection and data handling, Chromeleon software v. 6.80 was used. Preparative HPLC was carried out on an Agilent Prep HPLC systems with Agilent 1100 series pump, Agilent 1200 series diode array, multiple wavelength detector (G1365B), and Agilent PrepHT High Performance Preparative Cartridge Column (Zorba× 300 SB-C18 Prep HT, 21.2 × 250 mm, 7 μm). LC-MS spectra were recorded using either an Agilent 1200 series solvent delivery system equipped with an autoinjector coupled to an Agilent 6400 series triple quadrupole mass spectrometer equipped with an electrospray ionization source or Waters Aquity UPLC-MS with dual wavelength detection with electrospray ionization. Gradients of 5% aqueous MeCN + 0.1% HCO_2H (solvent A), and 95% aqueous MeCN + 0.05% HCO_2H (solvent B) were employed. IR spectra were recorded on a Perkin-Elmer 801 spectrophotometer. Optical rotation was measured

using a Perkin-Elmer 241 Spectrometer or an Anton Paar Modular Circular Polarimeter (MCP) 100/150 with Na lamp (D line, 589 nm). Compounds were dried under high vacuum or freeze-dried using a Holm & Halby, Heto LyoPro 6000 freeze drier. The purity of compounds submitted for pharmacological characterization was determined by HPLC to be >95%.

Ethyl (1*S*,2*S*)-2-((benzyloxy)methyl)cyclopropane-1-carboxylate (6). To a solution of triethylphosphonoacetate (1.3 mL, 6.6 mmol) in dimethoxyethane (10 mL) was added *n*-BuLi (3.1 mL, 2.15 M in toluene) dropwise over 15 min under ice bath and an argon atmosphere. After stirring at rt for 15 min, *S*-benzylglycidyl ether (**5**, 0.5 mL, 3.3 mmol) was added dropwise, followed by heating at 130 °C for 16 h. The solution was cooled to rt, diluted with EtOAc (500 mL), then washed with sat. NH_4Cl solution (250 mL). After drying over $MgSO_4$ and concentration in vacuum, the crude product was purified by flash chromatography to give the title compound **6**, as a colorless oil (582 mg, 75%). ^{1}H NMR (600 MHz, Chloroform-*d*) δ 7.37 – 7.31 (m, 4H), 7.30 – 7.27 (m, 1H), 4.52 (s, 2H), 4.12 (qq, *J* = 3.72, 7.21 Hz, 2H), 3.45 (dd, *J* = 6.02, 10.36 Hz, 1H), 3.37 (dd, *J* = 6.53, 10.37 Hz, 1H), 1.74 (ddd, *J* = 4.06, 6.39, 8.93 Hz, 1H), 1.57 (ddd, *J* = 3.99, 4.80, 8.63 Hz, 1H), 1.26 (t, *J* = 7.14 Hz, 3H), 1.21 (dt, *J* = 4.48, 8.95 Hz, 1H), 0.86 (ddd, *J* = 4.23, 6.25, 8.35 Hz, 1H).

(1*S*,2*S*)-2-((Benzyloxy)methyl)cyclopropane-1-carboxylic acid (**7**). To a solution of **6** (286 mg, 1.22 mmol) in THF (10 mL) was added aqueous NaOH (102 mg, 2.56 mmol) in water (6.3 mL) over 5 min. The reaction mixture was then stirred at rt for overnight. The resulting mixture was diluted with water (100 mL), acidified to pH= 4 with 1 M HCl, then extracted with EtOAc (3 × 50 mL). Organic extracts were combined, dried over $MgSO_4$ and concentrated in vacuum to afford the desired colorless oil **7** (252 mg, quant.); ^{1}H NMR (400 MHz, Chloroform-*d*) δ 7.38 – 7.27 (m, 5H), 4.53 (s, 2H), 3.48 (dd, *J* = 5.85, 10.42 Hz, 1H), 3.37 (dd, *J* = 6.48, 10.43 Hz, 1H), 1.80 (ddd, *J* = 3.73, 6.27, 9.61 Hz, 1H), 1.58 (dt, *J* = 4.43, 8.57 Hz, 1H), 1.28 (dt, *J* = 4.53, 9.05

Hz, 1H), 0.98 – 0.89 (m, 1H). ^{13}C NMR (101 MHz, $CDCl_3$) δ 179.8, 138.0, 128.4, 127.7, 127.7, 72.7, 71.2, 22.5, 18.3, 13.6.

(1*S*,2*S*)-2-((Benzyloxy)methyl)-*N*-(quinolin-8-yl)cyclopropane-1-carboxamide (8). A mixture of **7** (1.66 g, 8.04 mmol), EDCI (1.85 g, 9.65 mmol), and HOBt (1.30 g, 9.65 mmol), in anhydrous DCM (20 mL) was stirred at rt. After 0.5 h, 8-aminoquinoline (1.39 g, 9.65 mmol) was added, and the reaction mixture was stirred at rt for 2 d. The mixture was washed with 1 M HCl, water and brine. The organic layer was dried over $MgSO_4$ and concentrated in vacuum. The residue was purified by flash chromatography to give the desired product **8** as a pale brown oil (1.82 g, 68%). ^{1}H NMR (400 MHz, Chloroform-*d*) δ 10.02 (s, 1H), 8.81 (dd, *J* = 1.67, 4.28 Hz, 1H), 8.73 (dd, *J* = 1.75, 7.23 Hz, 1H), 8.16 (dd, *J* = 1.68, 8.29 Hz, 1H), 7.57 – 7.43 (m, 3H), 7.40 – 7.26 (m, 5H), 4.57 (d, *J* = 1.71 Hz, 2H), 3.59 (dd, *J* = 5.86, 10.43 Hz, 1H), 3.47 (dd, *J* = 6.51, 10.41 Hz, 1H), 1.91 (dqd, *J* = 3.95, 6.19, 8.89 Hz, 1H), 1.78 (dt, *J* = 4.39, 8.51 Hz, 1H), 1.39 (dt, *J* = 4.47, 8.94 Hz, 1H), 0.95 (ddd, *J* = 4.19, 6.23, 8.19 Hz, 1H). ^{13}C NMR (101 MHz, $CDCl_3$) δ 171.1, 148.0, 138.2, 136.4, 134.6, 128.4, 128.0, 127.7, 127.7, 127.5, 121.6, 121.3, 116.5, 72.6, 71.5, 21.9, 21.4, 12.8.

Ethyl 2-((1*S*,2*S*,3*S*)-2-((benzyloxy)methyl)-3-(quinolin-8-ylcarbamoyl)cyclopropyl)acetate (9). To a mixture of **8** (500 mg, 1.50 mmol), AgOAc (551 mg, 3.3 mmol), and $Pd(OAc)_2$ (67 mg, 0.3 mmol) in anhydrous toluene (5.0 mL), ethyl iodoactetate (534 μL, 4.5 mmol) was added under an argon atmosphere. The reaction mixture was allowed to stir at 110 °C for 3 d. The reaction mixture was filtered through a pad of celite after cooled to rt and rinsed with EtOAc. The filtrate was concentrated and the crude was purified by flash chromatography to give the desired product **9** as a colorless oil (290 mg, 46%). ^{1}H NMR (600 MHz, Chloroform-*d*) δ 10.04 (s, 1H), 8.80 (dd, *J* = 1.68, 4.21 Hz, 1H), 8.72 (dd, *J* = 1.56, 7.42 Hz, 1H), 8.15 (dd, *J* = 1.66, 8.24 Hz, 1H), 7.53 – 7.47 (m, 2H), 7.45 (dd, *J* = 4.21, 8.25 Hz, 1H), 7.36 – 7.33 (m, 4H), 7.30 – 7.26 (m, 1H), 4.56 (d, *J* = 2.19 Hz, 2H), 4.03 (p, *J* = 7.10 Hz, 2H), 3.62 (dd, *J* = 5.63, 10.41 Hz,

1H), 3.54 (dd, *J* = 6.05, 10.43 Hz, 1H), 2.84 (dd, *J* = 6.51, 17.01 Hz, 1H), 2.76 (dd, *J* = 7.90, 17.02 Hz, 1H), 1.99 (dd, *J* = 4.86, 8.78 Hz, 1H), 1.96 – 1.91 (m, 1H), 1.67 (ddd, *J* = 1.74, 5.16, 8.39 Hz, 1H), 1.10 (t, *J* = 7.13 Hz, 3H).

Ethyl 2-((1*S*,2*S*,3*S*)-2-(hydroxymethyl)-3-(quinolin-8-ylcarbamoyl)cyclopropyl)acetate (10). To a solution of **9** (500 mg, 1.50 mmol) in anhydrous DCM (5.0 mL) was added BCl_3 (8.46 mL, 8.46 mmol, 1.0 M in hexanes) dropwise at -78 °C under an argon atmosphere. The reaction was kept stirring at the same temperature for 1.5 h. Then, the mixture was allowed to stir at 0 °C for 15 min, $NaHCO_3$ was added at -78 °C. The reaction mixture was warmed to rt and stirred for 4 h and quenched by water. The separated organic phase was washed with brine, dried over $MgSO_4$ and concentrated in vacuum. The crude was purified by flash chromatography to give the desired product **10** as a colorless oil (282 mg, 61%). ^{1}H NMR (400 MHz, Chloroform-*d*) δ 10.05 (s, 1H), 8.80 (dd, *J* = 1.69, 4.24 Hz, 1H), 8.71 (dd, *J* = 2.14, 6.85 Hz, 1H), 8.16 (dd, *J* = 1.67, 8.36 Hz, 1H), 7.56 – 7.42 (m, 3H), 4.11 (ddd, *J* = 1.60, 5.55, 7.13 Hz, 2H), 3.96 – 3.87 (m, 1H), 3.46 (ddd, *J* = 2.61, 8.09, 11.04 Hz, 1H), 2.88 (dd, *J* = 8.82, 17.68 Hz, 1H), 2.73 (dd, *J* = 5.93, 17.67 Hz, 1H), 2.40 (dd, *J* = 3.56, 7.33 Hz, 1H), 1.98 (dd, *J* = 4.87, 8.74 Hz, 1H), 1.95 – 1.89 (m, 1H), 1.55 (tt, *J* = 6.16, 8.77 Hz, 1H), 1.19 (t, *J* = 7.13 Hz, 3H). ^{13}C NMR (101 MHz, $CDCl_3$) δ 173.7, 168.8, 148.1, 138.2, 136.4, 134.5, 127.9, 127.4, 121.6, 121.4, 116.3, 64.7, 60.7, 30.9, 28.4, 26.0, 22.1, 14.1.

Ethyl 2-((1*S*,2*S*,3*S*)-2-formyl-3-(quinolin-8-ylcarbamoyl)cyclopropyl)acetate (11). To an ice-cooled stirred solution of **10** (180 mg, 0.548 mmol) in DCM (4.0 mL) was added Dess-Martin periodinane (349 mg, 0.822 mmol). The resultant mixture was allowed to warm to rt for overnight. The mixture was diluted with DCM, quenched with a 1: 1 solution of sat. $NaHCO_3$ and sat.$Na_2S_2O_3$ (12.0 mL). After vigorous stirring for 0.5 h, the mixture was separated. The organic phase was washed with brine, dried over $MgSO_4$ and concentrated in vacuum. The crude was purified by flash chromatography to give the desired product **11** as a colorless oil (107 mg, 60%).

^{1}H NMR (600 MHz, Chloroform-*d*) δ 10.14 (s, 1H), 9.62 (d, *J* = 3.06 Hz, 1H), 8.79 (dd, *J* = 1.67, 4.23 Hz, 1H), 8.69 – 8.63 (m, 1H), 8.14 (dd, *J* = 1.68, 8.24 Hz, 1H), 7.54 – 7.47 (m, 2H), 7.44 (dd, *J* = 4.20, 8.24 Hz, 1H), 4.09 – 4.02 (m, 2H), 2.87 (qd, *J* = 7.27, 17.23 Hz, 2H), 2.76 – 2.68 (m, 2H), 2.24 (dtd, *J* = 5.92, 7.25, 9.16 Hz, 1H), 1.13 (t, *J* = 7.14 Hz, 3H). ^{13}C NMR (151 MHz, $CDCl_3$) δ 198.4, 171.7, 166.2, 148.3, 138.2, 136.3, 134.2, 127.9, 127.2, 121.9, 121.7, 116.5, 77.3, 77.1, 76.9, 60.7, 35.0, 30.9, 30.1, 25.4, 14.0.

Ethyl 2-((1*S*,2*S*,3*S*)-2-(cyano(((*R*)-2-hydroxy-1-phenylethyl)amino)methyl)-3-(quinolin-8-ylcarbamoyl)cyclopropyl)acetate (12). To a solution of **11** (277 mg, 0.85 mmol) in anhydrous MeOH (4.0 mL) was added (*R*)-α-phenylglycinol (151 mg, 1.10 mmol) under an argon atmosphere. The resultant solution was stirred at rt for 3 h and then trimethylsiyl cyanide (0.212 mL, 1.70 mmol) was added dropwise at 0 °C. The reaction mixture was stirred at rt for overnight. The solvent was removed in vacuum to afford the crude, which was purified by flash chromatography to give the desired product **12** as a colorless oil (250 mg, 62%). ^{1}H NMR (400 MHz, Chloroform-*d*) δ 10.08 (s, 1H), 8.82 (dd, *J* = 1.66, 4.26 Hz, 1H), 8.67 (dd, *J* = 3.69, 5.28 Hz, 1H), 8.16 (dd, *J* = 1.68, 8.30 Hz, 1H), 7.54 – 7.50 (m, 2H), 7.47 (dd, *J* = 4.23, 8.27 Hz, 1H), 7.42 – 7.28 (m, 5H), 4.18 – 4.10 (m, 3H), 3.82 (dd, *J* = 4.14, 10.97 Hz, 1H), 3.76 – 3.65 (m, 2H), 2.86 (dd, *J* = 8.82, 17.61 Hz, 1H), 2.73 (dd, *J* = 5.77, 17.62 Hz, 1H), 2.15 (dd, *J* = 5.00, 9.17 Hz, 1H), 2.10 – 2.04 (m, 1H), 1.82 (tt, *J* = 6.10, 8.92 Hz, 1H), 1.20 (t, *J* = 7.11 Hz, 3H). ^{13}C NMR (101 MHz, $CDCl_3$) δ 172.8, 167.5, 148.3, 138.1, 138.1, 136.4, 134.3, 128.9, 128.4, 127.9, 127.8, 127.3, 121.7, 121.7, 117.5, 116.4, 77.3, 77.0, 76.7, 67.6, 63.0, 60.8, 49.9, 30.9, 26.6, 25.4, 20.7, 14.1.

(1*S*,2*S*,3*S*)-2-((*S*)-Amino(carboxy)methyl)-3-(carboxymethyl)cyclopropane-1-carboxylic acid (LBG30300). To a solution of **12** (150 mg, 0.34 mmol) in anhydrous DCM/MeOH (9.0 mL, 1:1) was added $Pb(OAc)_4$ (317 mg, 0.714 mmol) at 0 °C. After stirring for 10 min, H_2O (9.0 mL) was added. The mixture was filtered through a pad of celite and the filtrate was concentrated to

get the crude intermediate. To the resultant crude was added 6 M HCl (4.2 mL) and allowed to heat to 110 ºC for overnight. The crude product was purified by preparative HPLC and the combined fractions were treated with 1 M HCl to give **LBG30300** as the HCl salt (14 mg, 20%). Purity: ≥ 95%, Rt: 2.82 min. ^{1}H NMR (600 MHz, Deuterium Oxide) δ 3.66 (d, *J* = 10.02 Hz, 1H), 2.91 (dd, *J* = 6.22, 17.26 Hz, 1H), 2.64 (dd, *J* = 8.70, 17.27 Hz, 1H), 2.18 (dd, *J* = 4.97, 9.39 Hz, 1H), 2.03 (tt, *J* = 6.25, 9.02 Hz, 1H), 1.89 (ddd, *J* = 5.02, 6.27, 10.21 Hz, 1H). ^{13}C NMR (101 MHz, D_2O) δ 176.3, 174.3, 170.7, 55.3, 31.2, 26.3, 23.6, 22.4. LC-MS (*m/z*) calcd. for $C_8H_{13}NO_6$ $[M+H]^+$, 218.2; found, 218.1. $[\alpha]_D^{25}$ +6.21 (*c* 0.102, H_2O).

Pharmacology

Cell Culture and Transfection. HEK293 cells were transiently transfected with rat mGlu receptors encoding plasmids by electroporation and cultured in Dulbecco's modified Eagle's medium (Life Technologies,Cergy Pontoise, France) supplemented with 10% of fetal bovine serum. Cells were seeded in polyornithine-coated 96-well plates at a density of 150 000 cells/well. In order to minimize extracellular Glu concentration, receptors were cotransfected with the high-affinity Glu transporter EAAC1 and medium was replaced by Glutamax DMEM (Life Technologies) without serum at least 2h before running the experiments.

IP-One Functional Assay. To monitor receptor signalling activity through inositol monophosphate (IP1) production, group II and group III mGlu receptors were cotransfected with the chimeric Gqi9 protein to allow coupling to the phospholipase C pathway. Twenty-four hours after transfection, cells were washed with Krebs buffer, and stimulated for 30 min with the indicated compounds in the presence of LiCl (50 mM). IP1 production was determined using the IP-One HTRF kit (Cisbio Biossays, Codolet, France) according to the manufacturer's recommendations. For $mGlu_3$, cells were first incubated with 1 μM **LY341495** for 10 min at 37 °C in Krebs buffer. Then, cells were washed two times with Krebs buffer and stimulated with the

indicated concentrations of compounds. However, in order to circumvent the lowering of the observed agonist EC50s by the remaining antagonist compounds, we determined a correction factor. This factor was calculated as the ratio of the EC_{50}s (9.54 ± 1.95) of the compounds on $mGlu_2$, determined in the same two conditions, with and without the preincubation with 1 μM of the antagonist **LY341495**. The EC_{50}s presented for $mGlu_3$ in **Table 1** are were determined by applying this correction factor to the measured EC_{50}s. Experiments were performed at least in duplicates, and data were analysed using Prism software (GraphPad, La Jolla, CA, USA).

Fluorescence labeling and TR-FRET measurements. SNAP-tag labeling was performed as described previously.[41] Briefly, 24h after transfection, HEK293 cells were incubated at 37℃ for 1h with a solution of 100 nM of SNAP-Lumi4-Tb, 60 nM of SNAP-Green. Cells were then washed three times with Krebs buffer, and drugs were added. The TR-FRET measurements were performed on a PHERAstar FS microplate reader (BMG Labtech, Ortenberg, Germany) equipped with 'TR-FRET' optical modules and two photomultiplier tubes to detect two emission wavelengths corresponding to the donor and acceptor emission, simultaneously.[41] To monitor the emissive decay curves, the Lumi4-Tb present in each well was excited using N2 laser emission line at 337 nm (40 flashes per well for the 96-well plate format, 20 flashes per well for the 384-well plate format). The emission decay was collected during 2500 or 5000 ms with 5 ms or 10 ms steps, respectively, at 620 nm for the donor (Lumi4-Tb) and at 520 nm for Green. The optimal acceptor ratio was determined as previously reported,[41] and calculated using the sensitized acceptor signal integrated over the time window [50 ms- 100 ms], divided by the sensitized acceptor signal integrated over the time window [800 ms-1200 ms]. As described above for the IP-One assay, to circumvent the shift of the EC50s determined on $mGlu_3$ after a pre-incubation with the antagonist (1 μM), similar experiments were conducted on $mGlu_2$ in order to determine the EC50s on $mGlu_2$ in identical conditions, meaning after preincubation of antagonist (1 μM) and washing. This is presented in Table 3.

Molecular Modelling

Docking (design)

Induced fit docking was carried out in MOE (2022.02) using standard setup with AMBER-10 EHT as the forcefield. The protein ($mGlu_2$, pdb code 5cni) was prepared for docking by applying the build-in function "Protonate-3D" under standard parameters. Binding modes were returned with a scoring function *S* in kcal/mol. Best poses were selected here from.

Docking (subtype selectivity study)

In order to computationally investigate the selectivity of **LBG30300** towards $mGlu_2$, several docking experiments were performed using Gold[43] as implemented in Discovery Studio (Dassault Systèmes BIOVIA. *Discovery Studio Modeling Environment, Release 2021*; Dassault Systèmes: San Diego, 2021). **LBG30300** was sketched then prepared using the prepare ligands protocol in Discovery Studio (Dassault Systèmes BIOVIA, Discovery Studio, 2021, San Diego: Dassault Systèmes) followed by ligand minimization using CHARMm forcefield. For docking at $mGlu_2$, the crystallized structure (PDB ID: 5CNJ)[29] was selected due to the presence of different conformations of Tyr144 at the orthosteric binding site as revealed by the flip of Tyr144 in chain A which was not observed in chain B. Hence, a flexible docking in $mGlu_2$ chain A was performed. Binding constraints were set to ensure that top poses have the glutamate-like interactions.[12] Thr168 and Ser145 were selected as hydrogen bond donors whereas Arg61 was selected as a hydrogen bond acceptor. Additionally, five residues in the vicinity of the ligand were selected for flexibility during docking: Lys43, Arg57, Tyr144, Ser272, and Arg271. The maximum number of poses was set to 100, with an early termination at three poses if the RMSD was less than 1.5 Angstrom successively. Then a docking experiment in $mGlu_2$ chain B was carried out. This docking had the same parameters

as the one described above for chain A. Furthermore, two docking experiments were performed, one in $mGlu_8$ and the other in $mGlu_3$, using PDB IDs 6BSZ, and 4XAR as templates respectively. Likewise, the same parameters were set with different residues.

Molecular Dynamics

Following the pose selection of the docking of **LGB30300** in $mGlu_2$ chain A. The stability of the complex was assessed by molecular dynamics simulations using Discovery Studio (Dassault Systèmes BIOVIA. *Discovery Studio Modeling Environment, Release 2021*; Dassault Systèmes: San Diego, 2021) and NAMD[45] implemented in Discovery studio. First, the complex was typed with charmm36[46] force field then was placed in an orthorhombic box at a minimum distance of 10 Å from the boundary and solvated with TIP3 water model. Na^+ and Cl^- were added to maintain a salt concentration of 0.145 M. The system was then minimized and equilibrated using the standard Dynamics Cascade protocol. Then three production replicates were launched for 10 ns each in NPT ensemble at 300K using Langevin thermostat for temperature control. Likewise, molecular dynamics of the chosen pose of the docking of **LGB30300** and $mGlu_8$ complex were launched for 10 ns. For pose selection, same system trajectories were concatenated then ttclust[47] was used to clusterize the frames. The frame representing the most abundant cluster was selected.

AUTHOR INFORMATION

Corresponding Author: Lennart Bunch, email: lebu@sund.ku.dk, Phone, +45 35 33 62 44

ACKNOWLEDGMENTS

The authors gratefully acknowledge the financial support from the Danish Research Council (DFF/FSS) and the China Scholarship Council (CSC) foundation. F.A. was supported by the

Science Ambassador Program from Dassault Systèmes BIOVIA and F.E by the Agence Nationale de la Recherche (ANR 2020 NANO4SCHIZO).

ABBREVIATIONS USED

CNS, central nervous system; iGluRs, ionotropic Glu receptors; mGlu receptors, metabotropic Glu receptors; GPCRs, G protein-coupled receptors; CCG, *L*-2-(carboxycyclopropyl)glycine; carboxycyclopropyl alanines; NAMD, not another molecular dynamics program; PDB, protein data bank; RMSD, root mean square deviation; LY354740, (1*S*,2*S*,5*R*,6*S*)-2-aminobicyclo[3.1.0]hexane-2,6-dicarboxylate; LY2794193, (1*S*,2*S*,4*S*,5*R*,6*S*)-2-amino-4-[(3-methoxybenzoyl)amino]bicyclo[3.1.0]hexane-2,6-dicarboxylic acid; LY281223, (1*R*,2*S*,4*R*,5*R*,6*R*)-2-amino-4-(1H-1,2,4-triazol-3-ylsulfanyl)-bicyclo[3.1.0]hexane-2,6-dicarboxylic acid; AP4, 2-amino-4-phosphonobutyric acid; VFT, venus flytrap.

Supporting Information Availability

NMR spectra of **LBG30300** and intermediates. HPLC purity traces of **LBG30300**. **Table S1**: Alignment of group and subtype selective residues in the glutamate binding site of the mGlu receptors. **Figure S1:** Docking of **LBG30300** in the $mGlu_2$-VFT. **Figure S2**: Docking of **LBG300** in the $mGlu_2$-VFT. **Figure S3:** Docking of **LBG30300** in the $mGlu_8$-VFT receptor binding site. PDB files of **LBG30300** docked into mGlu2-VFT (Figure 8) and into $mGlu_8$-VFT (Figure 9). Animal in vivo study: Method and data collection protocols.

REFERENCES

(1) Parpura, V.; Basarsky, T. A.; Liu, F.; Jeftinija, K.; Jeftinija, S.; Haydon, P. G. Glutamate-Mediated Astrocyte–Neuron Signalling. *Nature* **1994**, *369* (6483), 744–747. https://doi.org/10.1038/369744a0.

(2) Ozawa, S.; Kamiya, H.; Tsuzuki, K. Glutamate Receptors in the Mammalian Central Nervous System. *Prog Neurobiol* **1998**, *54* (5), 581–618.

(3) Gereau, R. W.; Swanson, G. *The Glutamate Receptors*; Springer Science & Business Media, 2008.

(4) Willard, S. S.; Koochekpour, S. Glutamate, Glutamate Receptors, and Downstream Signaling Pathways. *Int J Biol Sci* **2013**, *9* (9), 948–959. https://doi.org/10.7150/ijbs.6426.

(5) Niswender, C. M.; Conn, P. J. Metabotropic Glutamate Receptors: Physiology, Pharmacology, and Disease. *Annu Rev Pharmacol Toxicol* **2010**, *50*, 295–322. https://doi.org/10.1146/annurev.pharmtox.011008.145533.

(6) Petralia, R. S.; Wang, Y.-X.; Niedzielski, A. S.; Wenthold, R. J. The Metabotropic Glutamate Receptors, MGluR2 and MGluR3, Show Unique Postsynaptic, Presynaptic and Glial Localizations. *Neuroscience* **1996**, *71* (4), 949–976.

(7) Tamaru, Y.; Nomura, S.; Mizuno, N.; Shigemoto, R. Distribution of Metabotropic Glutamate Receptor MGluR3 in the Mouse CNS: Differential Location Relative to Pre- and Postsynaptic Sites. *Neuroscience* **2001**, *106* (3), 481–503.

(8) Neki, A.; Ohishi, H.; Kaneko, T.; Shigemoto, R.; Nakanishi, S.; Mizuno, N. Pre-and Postsynaptic Localization of a Metabotropic Glutamate Receptor, MGluR2, in the Rat Brain: An Immunohistochemical Study with a Monoclonal Antibody. *Neurosci Lett* **1996**, *202* (3), 197–200.

(9) Corti, C.; Battaglia, G.; Molinaro, G.; Riozzi, B.; Pittaluga, A.; Corsi, M.; Mugnaini, M.; Nicoletti, F.; Bruno, V. The Use of Knock-out Mice Unravels Distinct Roles for MGlu2

and MGlu3 Metabotropic Glutamate Receptors in Mechanisms of Neurodegeneration/Neuroprotection. *Journal of Neuroscience* **2007**, *27* (31), 8297–8308.

(10) Higgins, G. A.; Ballard, T. M.; Kew, J. N. C.; Richards, J. G.; Kemp, J. A.; Adam, G.; Woltering, T.; Nakanishi, S.; Mutel, V. Pharmacological Manipulation of MGlu2 Receptors Influences Cognitive Performance in the Rodent. *Neuropharmacology* **2004**, *46* (7), 907–917.

(11) Morishima, Y.; Miyakawa, T.; Furuyashiki, T.; Tanaka, Y.; Mizuma, H.; Nakanishi, S. Enhanced Cocaine Responsiveness and Impaired Motor Coordination in Metabotropic Glutamate Receptor Subtype 2 Knockout Mice. *Proceedings of the National Academy of Sciences* **2005**, *102* (11), 4170–4175.

(12) Acher, F. C.; Cabayé, A.; Eshak, F.; Goupil-Lamy, A.; Pin, J. P. Metabotropic Glutamate Receptor Orthosteric Ligands and Their Binding Sites. *Neuropharmacology* **2022**, *204*, 108886. https://doi.org/10.1016/J.NEUROPHARM.2021.108886.

(13) Hao, J.; Chen, Q. Insights into the Structural Aspects of the MGlu Receptor Orthosteric Binding Site. *Current Topic in Medicinal Chemistry* **2019**, *19* (26), 2421–2446. https://doi.org/10.2174/1568026619666191011094935.

(14) Tora, A. S.; Rovira, X.; Cao, A. M.; Cabaye, A.; Olofsson, L.; Malhaire, F.; Scholler, P.; Baik, H.; Van Eeckhaut, A.; Smolders, I.; Rondard, P.; Margeat, E.; Acher, F.; Pin, J. P.; Goudet, C. Chloride Ions Stabilize the Glutamate-Induced Active State of the Metabotropic Glutamate Receptor 3. *Neuropharmacology* **2018**, *140*, 275–286. https://doi.org/10.1016/j.neuropharm.2018.08.011.

(15) Ma, D. Conformationally Constrained Analogues OfL-Glutamate as Subtype-Selective Modulators of Metabotropic Glutamate Receptors. *Bioorg Chem* **1999**, *27* (1), 20–34.

(16) Acher, F. C. Metabotropic Glutamate Receptors. *Tocris Biosci. Rev. Lett* **2019**, 1–24.

(17) Palmer, E.; Monaghan, D. T.; Cotman, C. W. Trans-ACPD, a Selective Agonist of the Phosphoinositide-Coupled Excitatory Amino Acid Receptor. *Eur J Pharmacol* **1989**, *166* (3), 585–587.

(18) Schoepp, D. D.; Johnson, B. G.; Salhoff, C. R.; McDonald, J. W.; Johnston, M. V. In Vitro and In Vivo Pharmacology of Trans- and Cis-(±)-1-Amino-1,3-Cyclopentanedicarboxylic Acid: Dissociation of Metabotropic and Ionotropic Excitatory Amino Acid Receptor Effects. *J Neurochem* **1991**, *56* (5), 1789–1796. https://doi.org/10.1111/j.1471-4159.1991.tb02082.x.

(19) Yamanoi, K.; Ohfune, Y.; Watanabe, K.; Li, P. N.; Takeuchi, H. Synthesis of Trans and Cis-α-(Carboxycyclopropyl) Glycines. Novel Neuroinhibitory Amino Acids as L-Glutamate Analogue. *Tetrahedron Lett* **1988**, *29* (10), 1181–1184.

(20) Shimamoto, K.; Ohfune, Y. Syntheses and Conformational Analyses of Glutamate Analogs: 2-(2-Carboxy-3-Substituted-Cyclopropyl) Glycines as Useful Probes for Excitatory Amino Acid Receptors. *J Med Chem* **1996**, *39* (2), 407–423.

(21) Hayashi, Y.; Tanabe, Y.; Aramori, I.; Masu, M.; Shimamoto, K.; Ohfune, Y.; Nakanishi, S. Agonist Analysis of 2-(Carboxycyclopropyl)Glycine Isomers for Cloned Metabotropic Glutamate Receptor Subtypes Expressed in Chinese Hamster Ovary Cells. *Br J Pharmacol* **1992**, *107* (2), 539. https://doi.org/10.1111/J.1476-5381.1992.TB12780.X.

(22) Brabet, I.; Parmentier, M. L.; De Colle, C.; Bockaert, J.; Acher, F.; Pin, J. P. Comparative Effect of L-CCG-I, DCG-IV and γ-Carboxy-l-Glutamate on All Cloned Metabotropic Glutamate Receptor Subtypes. *Neuropharmacology* **1998**, *37* (8), 1043–1051. https://doi.org/10.1016/S0028-3908(98)00091-4.

(23) Collado, I.; Pedregal, C.; Mazón, A.; Espinosa, J. F.; Blanco-Urgoiti, J.; Schoepp, D. D.; Wright, R. A.; Johnson, B. G.; Kingston, A. E. (2 S, 1 ‘S, 2 ‘S, 3 ‘R)-2-(2 ‘-Carboxy-3 ‘-Methylcyclopropyl) Glycine Is a Potent and Selective Metabotropic Group 2 Receptor Agonist with Anxiolytic Properties. *J Med Chem* **2002**, *45* (17), 3619–3629.

(24) Collado, I.; Pedregal, C.; Bueno, A. B.; Marcos, A.; González, R.; Blanco-Urgoiti, J.; Pérez-Castells, J.; Schoepp, D. D.; Wright, R. A.; Johnson, B. G. (2 S, 1 ‘S, 2 ‘R, 3 ‘R)-2-(2 ‘-Carboxy-3 ‘-Hydroxymethylcyclopropyl) Glycine Is a Highly Potent Group 2 and 3 Metabotropic Glutamate Receptor Agonist with Oral Activity. *J Med Chem* **2004**, *47* (2), 456–466.

(25) Staudt, M.; Liu, N.; Malhaire Fanny; Prézeau, L.; Renard, E.; Hasanpour, Z.; Pin, J.-P.; Bunch, L. Synthesis and Pharmacological Characterization of Comformationally Restricted 2-Amino-Adipic Acid Analogs and Carboxycyclopropyl Glycines as Selective Metabotropic Glutamate 2 Receptor Agonists. *Eur J Med Chem* **2023**, *submitted*.

(26) Monn, J. A.; Valli, M. J.; Massey, S. M.; Wright, R. A.; Salhoff, C. R.; Johnson, B. G.; Howe, T.; Alt, C. A.; Rhodes, G. A.; Robey, R. L. Design, Synthesis, and Pharmacological Characterization of (+)-2-Aminobicyclo [3.1. 0] Hexane-2, 6-Dicarboxylic Acid (LY354740): A Potent, Selective, and Orally Active Group 2 Metabotropic Glutamate Receptor Agonist Possessing Anticonvulsant and Anxiolyti. *J Med Chem* **1997**, *40* (4), 528–537.

(27) Monn, J. A.; Valli, M. J.; Massey, S. M.; Hao, J.; Reinhard, M. R.; Bures, M. G.; Heinz, B. A.; Wang, X.; Carter, J. H.; Getman, B. G.; Stephenson, G. A.; Herin, M.; Catlow, J. T.; Swanson, S.; Johnson, B. G.; McKinzie, D. L.; Henry, S. S. Synthesis and Pharmacological Characterization of 4-Substituted-2-Aminobicyclo[3.1.0]Hexane-2,6-Dicarboxylates: Identification of New Potent and Selective Metabotropic Glutamate 2/3 Receptor Agonists. *J Med Chem* **2013**, *56* (11), 4442–4455. https://doi.org/10.1021/jm4000165.

(28) Monn, J. A.; Prieto, L.; Taboada, L.; Pedregal, C.; Hao, J.; Reinhard, M. R.; Henry, S. S.; Goldsmith, P. J.; Beadle, C. D.; Walton, L.; Man, T.; Rudyk, H.; Clark, B.; Tupper, D.; Baker, S. R.; Lamas, C.; Montero, C.; Marcos, A.; Blanco, J.; Bures, M.; Clawson, D. K.; Atwell, S.; Lu, F.; Wang, J.; Russell, M.; Heinz, B. A.; Wang, X.; Carter, J. H.; Xiang, C.;

Catlow, J. T.; Swanson, S.; Sanger, H.; Broad, L. M.; Johnson, M. P.; Knopp, K. L.; Simmons, R. M.; Johnson, B. G.; Shaw, D. B.; McKinzie, D. L. Synthesis and Pharmacological Characterization of C4-Disubstituted Analogs of 1S,2S,5R,6S-2-Aminobicyclo[3.1.0]Hexane-2,6-Dicarboxylate: Identification of a Potent, Selective Metabotropic Glutamate Receptor Agonist and Determination of Agonist-Bound Human. *J Med Chem* **2015**, *58* (4), 1776–1794. https://doi.org/10.1021/jm501612y.

(29) Monn, J. A.; Prieto, L.; Taboada, L.; Hao, J.; Reinhard, M. R.; Henry, S. S.; Beadle, C. D.; Walton, L.; Man, T.; Rudyk, H.; Clark, B.; Tupper, D.; Baker, S. R.; Lamas, C.; Montero, C.; Marcos, A.; Blanco, J.; Bures, M.; Clawson, D. K.; Atwell, S.; Lu, F.; Wang, J.; Russell, M.; Heinz, B. A.; Wang, X.; Carter, J. H.; Getman, B. G.; Catlow, J. T.; Swanson, S.; Johnson, B. G.; Shaw, D. B.; McKinzie, D. L. Synthesis and Pharmacological Characterization of C4-(Thiotriazolyl)-Substituted-2-Aminobicyclo[3.1.0]Hexane-2,6-Dicarboxylates. Identification of (1R,2S,4R,5R,6R)-2-Amino-4-(1H-1,2,4-Triazol-3-Ylsulfanyl)Bicyclo[3.1.0]Hexane-2, 6-Dicarboxylic Acid (LY281. *J Med Chem* **2015**, *58* (18), 7526–7548. https://doi.org/10.1021/acs.jmedchem.5b01124.

(30) Monn, J. A.; Henry, S. S.; Massey, S. M.; Clawson, D. K.; Chen, Q.; Diseroad, B. A.; Bhardwaj, R. M.; Atwell, S.; Lu, F.; Wang, J.; Russell, M.; Heinz, B. A.; Wang, X. S.; Carter, J. H.; Getman, B. G.; Adragni, K.; Broad, L. M.; Sanger, H. E.; Ursu, D.; Catlow, J. T.; Swanson, S.; Johnson, B. G.; Shaw, D. B.; McKinzie, D. L.; Hao, J. Synthesis and Pharmacological Characterization of C4beta-Amide-Substituted 2-Aminobicyclo[3.1.0]Hexane-2,6-Dicarboxylates. Identification of (1 S,2 S,4 S,5 R,6 S)-2-Amino-4-[(3-Methoxybenzoyl)Amino]Bicyclo[3.1.0]Hexane-2,6-Dicarboxylic Acid (LY2794193), a. *J Med Chem* **2018**, *61* (6), 2303–2328. https://doi.org/10.1021/acs.jmedchem.7b01481.

(31) Jullian, N.; Brabet, I.; Pin, J. P.; Acher, F. C. Agonist Selectivity of MGluR1 and MGluR2 Metabotropic Receptors: A Different Environment but Similar Recognition of an

Extended Glutamate Conformation. *J Med Chem* **1999**, *42* (9), 1546–1555. https://doi.org/10.1021/JM980571Q.

(32) Bessis, A.-S.; Jullian, N.; Coudert, E.; Pin, J.-P.; Acher, F. Extended Glutamate Activates Metabotropic Receptor Types 1, 2 and 4: Selective Features at MGluR4 Binding Site. *Neuropharmacology* **1999**, *38*, 1543–1551.

(33) Huynh, T. H. V. v; Erichsen, M. N.; Tora, A. S.; Goudet, C.; Sagot, E.; Assaf, Z.; Thomsen, C.; Brodbeck, R.; Stensbøl, T. B.; Bjørn-Yoshimoto, W. E.; Nielsen, B.; Pin, J. P.; Gefflaut, T.; Bunch, L. New 4-Functionalized Glutamate Analogues Are Selective Agonists at Metabotropic Glutamate Receptor Subtype 2 or Selective Agonists at Metabotropic Glutamate Receptor Group III. *J Med Chem* **2016**, *59* (3), 914–924. https://doi.org/10.1021/acs.jmedchem.5b01333.

(34) Armstrong, A.; Scutt, J. N. Stereocontrolled Synthesis of 3-(Trans-2-Aminocyclopropyl)Alanine, a Key Component of Belactosin A. *Org Lett* **2003**, *5* (13), 2331–2334. https://doi.org/10.1021/ol0346887.

(35) Jerhaoui, S.; Chahdoura, F.; Rose, C.; Djukic, J. P.; Wencel-Delord, J.; Colobert, F. Enantiopure Sulfinyl Aniline as a Removable and Recyclable Chiral Auxiliary for Asymmetric C(Sp(3))-H Bond Activation. *Chemistry (Easton)* **2016**, *22* (48), 17397–17406. https://doi.org/10.1002/chem.201603507.

(36) Collado, I.; Pedregal, C.; Bueno, A. B.; Marcos, A.; González, R.; Blanco-Urgoiti, J.; Pérez-Castells, J.; Schoepp, D. D.; Wright, R. a; Johnson, B. G.; Kingston, A. E.; Moher, E. D.; Hoard, D. W.; Griffey, K. I.; Tizzano, J. P. (2S,1'S,2'R,3'R)-2-(2'-Carboxy-3'-Hydroxymethylcyclopropyl) Glycine Is a Highly Potent Group 2 and 3 Metabotropic Glutamate Receptor Agonist with Oral Activity. *J Med Chem* **2004**, *47* (2), 456–466. https://doi.org/10.1021/jm030967o.

(37) Zhou, S.; Kern, E. R.; Gullen, E.; Cheng, Y.-C.; Drach, J. C.; Tamiya, S.; Mitsuya, H.; Zemlicka, J. 9-{[3-Fluoro-2-(Hydroxymethyl) Cyclopropylidene] Methyl} Adenines and-

Guanines. Synthesis and Antiviral Activity of All Stereoisomers. *J Med Chem* **2006**, *49* (20), 6120–6128.

(38) Felder, C. C.; Schober, D. A.; Tu, Y.; Quets, A.; Xiao, H.; Watt, M.; Siuda, E.; Nisenbaum, E.; Xiang, C.; Heinz, B.; Prieto, L.; McKinzie, D. L.; Monn, J. A. Translational Pharmacology of the Metabotropic Glutamate 2 Receptor-Preferring Agonist LY2812223 in the Animal and Human Brain. *J Pharmacol Exp Ther* **2017**, *361* (1), 190–197. https://doi.org/10.1124/JPET.116.237859.

(39) Monn, J. A.; Massey, S. M.; Valli, M. J.; Henry, S. S.; Stephenson, G. A.; Bures, M.; Hérin, M.; Catlow, J.; Giera, D.; Wright, R. A.; Johnson, B. G.; Andis, S. L.; Kingston, A.; Schoepp, D. D. Synthesis and Metabotropic Glutamate Receptor Activity of S-Oxidized Variants of (-)-4-Amino-2-Thiabicyclo-[3.1.0]Hexane-4,6-Dicarboxylate: Identification of Potent, Selective, and Orally Bioavailable Agonists for MGlu2/3 Receptors. *J Med Chem* **2007**, *50* (2), 233–240. https://doi.org/10.1021/JM060917U.

(40) Doumazane, E.; Scholler, P.; Fabre, L.; Zwier, J. M.; Trinquet, E.; Pin, J. P.; Rondard, P. Illuminating the Activation Mechanisms and Allosteric Properties of Metabotropic Glutamate Receptors. *Proc Natl Acad Sci U S A* **2013**, *110* (15), E1416–E1425. https://doi.org/10.1073/PNAS.1215615110/SUPPL_FILE/SAPP.PDF.

(41) Scholler, P.; Moreno-Delgado, D.; Lecat-Guillet, N.; Doumazane, E.; Monnier, C.; Charrier-Savournin, F.; Fabre, L.; Chouvet, C.; Soldevila, S.; Lamarque, L.; Donsimoni, G.; Roux, T.; Zwier, J. M.; Trinquet, E.; Rondard, P.; Pin, J. P. HTS-Compatible FRET-Based Conformational Sensors Clarify Membrane Receptor Activation. *Nature Chemical Biology 2017 13:4* **2017**, *13* (4), 372–380. https://doi.org/10.1038/nchembio.2286.

(42) Rorick-Kehn, L. M.; Perkins, E. J.; Knitowski, K. M.; Hart, J. C.; Johnson, B. G.; Schoepp, D. D.; McKinzie, D. L. Improved Bioavailability of the MGlu2/3 Receptor Agonist LY354740 Using a Prodrug Strategy: In Vivo Pharmacology of LY544344. *Journal of*

Pharmacology and Experimental Therapeutics **2006**, *316* (2), 905–913. https://doi.org/10.1124/JPET.105.091926.

(43) Jones, G.; Willett, P.; Glen, R. C.; Leach, A. R.; Taylor, R. Development and Validation of a Genetic Algorithm for Flexible Docking. *J Mol Biol* **1997**, *267* (3), 727–748. https://doi.org/10.1006/JMBI.1996.0897.

(44) Acher, F. C.; Bertrand, H. O. Amino Acid Recognition by Venus Flytrap Domains Is Encoded in an 8-Residue Motif. *Peptide Science* **2005**, *80* (2–3), 357–366. https://doi.org/10.1002/BIP.20229.

(45) Phillips, J. C.; Braun, R.; Wang, W.; Gumbart, J.; Tajkhorshid, E.; Villa, E.; Chipot, C.; Skeel, R. D.; Kalé, L.; Schulten, K. Scalable Molecular Dynamics with NAMD. *J Comput Chem* **2005**, *26* (16), 1781–1802. https://doi.org/10.1002/JCC.20289.

(46) Huang, J.; Rauscher, S.; Nawrocki, G.; Ran, T.; Feig, M.; De Groot, B. L.; Grubmüller, H.; MacKerell, A. D. CHARMM36m: An Improved Force Field for Folded and Intrinsically Disordered Proteins. *Nature Methods 2016 14:1* **2016**, *14* (1), 71–73. https://doi.org/10.1038/nmeth.4067.

(47) Tubiana, T.; Carvaillo, J. C.; Boulard, Y.; Bressanelli, S. TTClust: A Versatile Molecular Simulation Trajectory Clustering Program with Graphical Summaries. *J Chem Inf Model* **2018**, *58* (11), 2178–2182. https://doi.org/10.1021/ACS.JCIM.8B00512/SUPPL_FILE/CI8B00512_SI_001.PDF.

TOC

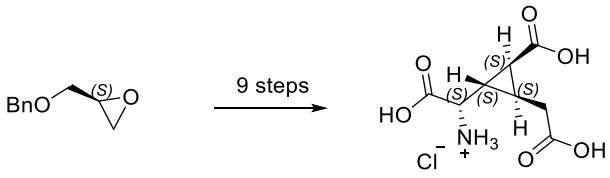

Commercially available enantiopure epoxide

LBG30300

EC$_{50}$ (nM)
mGlu2: 0.6
mGlu3: 372
mGlu1: >30.000
mGlu5: >30.000
mGlu4: 110
mGlu6: 280
mGlu8: 97